User Guide to the EFW measurements in the Cluster Active Archive (CAA)

prepared by

Per-Arne Lindqvist
Chris Cully
Yuri Khotyaintsev
Mats André
and the EFW team

1 Introduction

The four Cluster spacecraft were launched in two pairs on 16 July and 9 August 2000. Most of this user guide concerns the operations performed from 1 February 2001 to the end of scheduled science operations 30 September 2024. Section 5.3 concerns the commissioning period from launch to 31 January 2001. Spacecraft 2 re-entered the atmosphere as planned on 8 September 2024, spacecraft 1 will re-enter 2025 and the remaining two spacecraft during 2026.

The Cluster Active Archive (CAA) was created to archive all data from the Cluster mission. Emphasis is on providing the scientific community with calibrated science data. These data are now available in the Cluster Science Archie (CSA). This document describes the CAA/CSA data from the Electric Field and Waves (EFW) instrument. It gives some brief information on the instrument, followed by a description of the EFW science products available in the CAA/CSA. Some important things to keep in mind when using the data are given in the sections on caveats and quality parameters (Sections 5 and 6). For those interested, there is also a section describing some of the processing details (Appendix A).

2 Instrument Description

2.1 Instrument hardware

Details of the EFW instrument can be found in Gustafsson et al. [1997, 2001]. Here, some key characteristics useful for regular users are described briefly.

The detector of the instrument consists of four spherical sensors deployed orthogonally on 44 meter-long wire booms in the spin plane of the spacecraft. The configuration of the four probes of the EFW instrument in the spin plane is shown in Figure 1. The sun sensor is located between probes 2 and 3, 63.8 degrees from the $+Z_{SAT}$ axis. The potential difference between two opposing sensors, separated by 88 m tip-to-tip, is measured to provide an electric field measurement. Since there are four sensors, the full electric field in the spin plane is measured. The potential difference between each sensor and the spacecraft is measured separately (and is often used as a high time-resolution proxy for the ambient plasma density, [see Pedersen et al., 2008; André et al., 2015]). The potentials of the spherical sensor and nearby conductors (the so-called pucks and guards) are actively controlled in order to minimize errors associated with photoelectron fluxes to and from the spheres. The output signals from the spherical sensor preamplifiers are also provided to the wave instruments (STAFF, WHISPER and WBD) for analysis of high frequency wave phenomena.

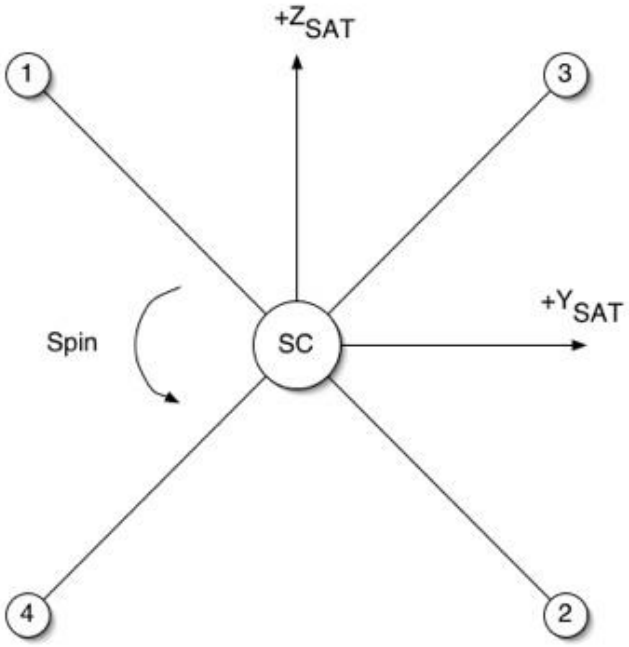

Figure 1: EFW probe configuration.

2.2 Probes and filters

EFW measures individual probe potentials with respect to the spacecraft with a sampling frequency of 5 s^{-1}, as well as the potential difference between selected probe pairs with a sampling frequency of 25 s^{-1} or 450 s^{-1} depending on the spacecraft telemetry mode (this can be seen in the CAA AUX TMMODE dataset).

Normally, the full spin plane electric field is computed using the orthogonal signals p12=p2-p1 and p34=p4-p3. However, several probes have failed during the mission lifetime:

Probe failures:

- probe 1, spacecraft 1: 28 December 2001
- probe 1, spacecraft 3: 29 July 2002
- probe 1, spacecraft 2: 13 May 2007
- probe 4, spacecraft 1: 19 April 2009 – 7 May 2009, and 14 October 2009
- probe 3, spacecraft 3: 1 June 2011
- probe 4, spacecraft 4: 1 July 2013
- probe 2, spacecraft 3: 3 November 2014
- probe 3, spacecraft 4: 17 February 2015
- probe 2, spacecraft 2: 12 October 2015
- probe 3, spacecraft 1: 10 December 2018
- probe 3, spacecraft 2: 23 August 2022
- probe 4, spacecraft 3: 28 April 2024

Due to a probe failure, the corresponding probe pair measurements are not available which has an impact on the quality of the full-resolution data. For instance, after probe 1 failed (spacecraft 1 on 28 Dec 2001; spacecraft 2 on 13 May 2007; spacecraft 3 on 29 Jul 2002), the signal p12 was no longer useful, but a workaround was implemented in the flight software to use p32 instead. This was fully implemented on 29 Sep 2003 on spacecraft 1 and 3, and on 24 Nov 2007 on spacecraft 2. In the intermediate period (Jan 2002 – Sep 2003 for SC1, Aug 2002 – Sep 2003 for SC3, and May – Nov 2007 for SC2), full resolution electric field data are generally not available. Probe 4 on spacecraft 4 failed on 1 Jul 2013 but the flight software could not be updated. The 4-second resolution electric field data are not affected, since it uses data from only one probe pair as input.

The failure of a second probe on a spacecraft meant the loss of any full resolution electric field data (spacecraft 1 probe 4 on 19 Apr 2009; spacecraft 3 probe 3 on 1 Jun 2011; spacecraft 4 probe 3 on 17 Feb 2015; spacecraft 2 probe 2 on 12 Oct 2015). Electric field data at 4-second resolution were still available on spacecraft 1, 2 and 4 (the remaining probes 2 and 4 on spacecraft 3 can not be used for electric field measurements).

The failure of a third probe on a spacecraft meant that routinely only spacecraft potential data could be obtained (spacecraft 3 probe 2 on 3 Nov 2014; spacecraft 1 probe 3 on 10 Dec 2018; spacecraft 2 probe 3 on 23 Aug 2022).

The failure of the last remaining fourth probe on a spacecraft meant that no EFW data could be obtained (spacecraft 3 probe 4 on 28 April 2024). (Note that during the last few days of scheduled science operations, 28 to 30 September 2024, data from STAFF and WHISPER (but not from EFW) are available).

A schematic overview of the relevant signal paths is given in Figure 2. The individual probe signals, p1 to p4, are normally routed through 7-pole low-pass filters with a cut-off frequency of 10 Hz before sampling. The probe difference signals, p12, p34 and p32 are normally routed through 10 Hz low-pass filters if sampled at 25 s^{-1}, and through 180 Hz low-pass filters when sampled at 450 s^{-1}.

The filters are normally connected to the sampled quantities as indicated in Figure 2. However, the 10 Hz filter on probe 3 on spacecraft 2 failed on 25 July 2001. As a workaround for this, the 180 Hz filter has been used for the difference signals sampled at both 450 s^{-1} and 25 s^{-1}. From 1 June 2007, all single probe signals on this spacecraft also use the 180 Hz filters. This has no effect on the 4 second resolution data, and only a marginal effect on the 25 s^{-1} data in those space environments where large amplitude electric field noise is present between 10 and 180 Hz.

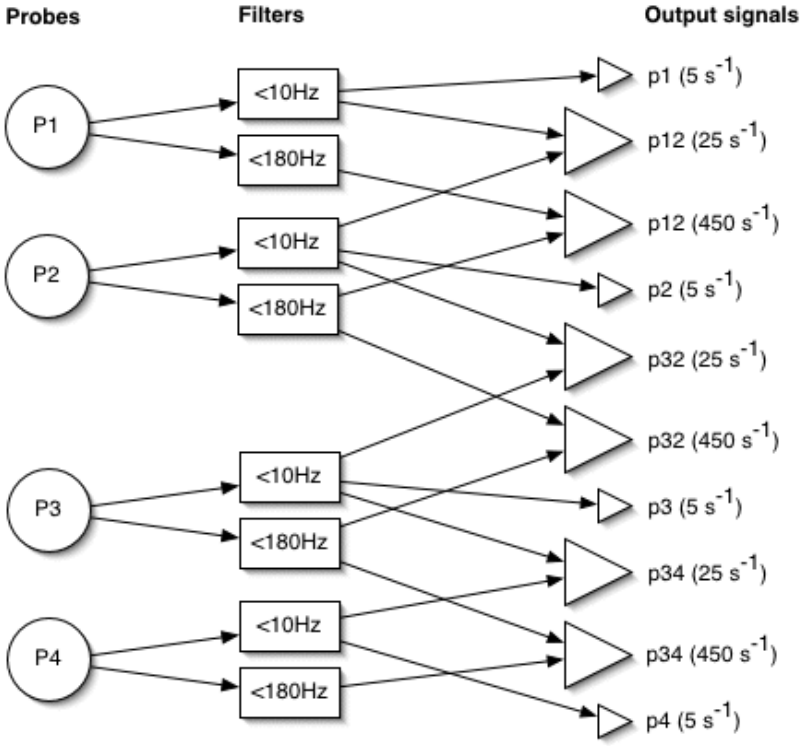

Figure 2: Probes, filters and sampled quantities.

2.3 Internal burst data

In addition to the nominal science data, EFW also collects high-resolution internal burst data into the internal 1Mb memory. Collection of the internal burst data is enabled during several hours each orbit. Typically there are two 10 second-long burst intervals decided by a specific burst trigger transmitted to ground. The burst duration is defined by the sampling frequency and the number of signals sampled. The bursts may contain up to 8 different signals sampled using two analog-to-digital convertors: single and differential probe electrical signals, magnetic signals provided by STAFF-SC search-coil sensors. The signals can be sampled using one of the following filters: 10 Hz, 180 Hz, 4kHz and 32 kHz low-pass filters as well as 8 kHz band pass filter, see Table 1 and Gustafsson et al. [1997]. Detailed information about the filter characteristics can be found in the Cluster EFW Filter Calibration Report [Stenberg, 2002]. The maximum sampling frequency is 36,000 s^{-1} for one signal, 18,000 s^{-1} for two signals, 9,000 s^{-1} for four signals and 4,500 s^{-1} for eight signals.

2.4 Time stamps of EFW data

The EFW data obtained at 5, 25 or 450 samples/s (Section 2.2) can normally be used without any correction of the time stamps attached to the data. EFW internal burst data with much higher sampling frequency (Section 2.3) may need correction of some of the time stamps before detailed use.

2.4.1 Time stamps of data in EFW internal burst mode

For use of the EFW internal burst data (Section 2.3), the time stamps of some data may need to be corrected: This is due to timing differences that may be present between nominally simultaneous EFW samples. This is due to EFW using two analog-to-digital converters (ADCs) operating at 36,000 samples/s. Each ADC gets its input signal from a multiplexor (MUX) at which various analog signals (quantities) can be selected. Not more than two quantities can therefore be sampled exactly simultaneously. For example, the four single probe signals (designated p1, p2, p3 and p4 in Figure 2) can therefore not all be simultaneously sampled: p1 and p2 are usually sampled first, then p3 and p4, with a time lag of 1/36,000 s (about 28 μs) between the two pairs.

The small timing difference can be important for the EFW internal burst data. When 4 signals (two pairs) are sampled at 9,000 samples/s, the timing difference between the first and second pair amounts to a 45 degree phase shift for a wave at the Nyqvist frequency (4,500 samples/s in this case) and correspondingly less for lower frequencies. The time stamp always refers to the first pair. The sampling order is specified in the file caveats. An example on how to find this information and how to correct the time stamps of EFW internal burst data are given below.

Example of Cluster 4 internal burst data CEF (Cluster Exchange Format) file format, for a period with 4 signals at 9,000 samples/s. The header and first three lines of data look as follows:

```
!-------------------- CEF ASCII FILE --------------------|
! created on 04-Sep-2014 09:11:16
!--------------------------------------------------------|
FILE_NAME = "C4_CP_EFW_L1_IB__20100930_V00.cef"
FILE_FORMAT_VERSION = "CEF-2.0"
END_OF_RECORD_MARKER = "$"
include = "CL_CH_MISSION.ceh"
include = "C4_CH_OBS.ceh"
include = "CL_CH_EFW_EXP.ceh"
include = "C4_CH_EFW_INST.ceh"
include = "C4_CH_EFW_L1_IB.ceh"
START_META     =   FILE_TYPE
   ENTRY       =   "cef"
END_META       =   FILE_TYPE
START_META     =   DATASET_VERSION
   ENTRY       =   "4"
END_META       =   DATASET_VERSION
START_META     =   LOGICAL_FILE_ID
   ENTRY       =   "C4_CP_EFW_L1_IB__20100930_V00"
END_META       =   LOGICAL_FILE_ID
START_META     =   VERSION_NUMBER
   ENTRY       =   "00"
END_META       =   VERSION_NUMBER
START_META     =   FILE_TIME_SPAN
   VALUE_TYPE  =   ISO_TIME_RANGE
   ENTRY       =   2010-09-30T00:00:00.000000Z/2010-10-01T00:00:00.000000Z
END_META       =   FILE_TIME_SPAN



START_META     =   GENERATION_DATE
   VALUE_TYPE  =   ISO_TIME
   ENTRY       =   2014-09-04T09:11:16.905079Z
END_META       =   GENERATION_DATE
START_META     =   FILE_CAVEATS
   ENTRY       =   "Data order: V1H V2H V3H V4H "
END_META       =   FILE_CAVEATS
!
!!!!!!!!!!!!!!!!!!!!!!!!!!!!!!!!!!!!!!!!!!!!!!!!!!!!!!!!
!                        Data                            !
!!!!!!!!!!!!!!!!!!!!!!!!!!!!!!!!!!!!!!!!!!!!!!!!!!!!!!!!
DATA_UNTIL = "END_OF_DATA"
2010-09-30T04:47:46.781820Z,  -11357,  -11352,  -11409,  -11386, -1000000000, -1000000000,
-1000000000, -1000000000 $
2010-09-30T04:47:46.781931Z,  -11357,  -11353,  -11410,  -11389, -1000000000, -1000000000,
-1000000000, -1000000000 $
2010-09-30T04:47:46.782042Z,  -11358,  -11353,  -11410,  -11389, -1000000000, -1000000000,
-1000000000, -1000000000 $
[...]
```

The last three lines of the file header contain the file caveats, which for the internal burst data files give the sampling order. The nomenclature in the file caveats can be decoded by using Table 1. Thus, the entry "V1H V2H V3H V4H" means the first sample pair is p1 and p2, with p3 and p4 sampled 1/36,000 s later. For each line in the data block, the time stamp is followed by the four signals in the order given in the file caveat, with the corresponding four quality flags terminating the line. (For details of the quality flags, see Section 6 and the CAA Interface Control Document for EFW.) The time stamp strictly applies only to the first pair of signals, while the actual time of the second pair is given by the time stamp plus 1/36,000 s ≈ 28 μs, e.g. 04:47:46.781848 for the last pair of samples on the first line.

For the common case of an internal burst with 8 quantities sampled at 4,500 samples/s, there are four pairs of data where the time stamp strictly applies to the first pair (as given by the file caveats) but 28 μs can be added to the time stamp of the second pair to get fully correct timing, 56 μs to the third pair, and 83 μs to the last pair.

A third common case is two signals at 18,000 samples/s. These are sampled simultaneously from analog quantities and the time stamps given are fully applicable.

Table 1. EFW internal burst data files

File caveat entry	Source	Low pass filter
VxL	px	10 Hz
VxM	px	180 Hz
VxyM	pxy	180 Hz
VxH	px	4 kHz
VxyH	pxy	Band pass up to 8 kHz
VxU	px	32 kHz
BSCq	STAFF SC signal	4 kHz

Table 1. Possible entries in the file caveats for EFW internal burst data files. Here x and y can be 1, 2, 3 or 4 (signifying EFW probes) and q can be X, Y or Z (denoting STAFF SC search-coil axes).

2.4.2 Time stamps of EFW data at 5 or 25 samples/s

The EFW data obtained at 5 or 25 samples/s (section 2.2) can be used without any correction of the time stamps.

The two E-field components in the spinning reference frame obtained at 25 samples/s, p12 and p34, are constructed onboard from the single probe signals and are therefore not exactly synchronized. As discussed in Section 2.4.1, there will be a time lag of about 28 μs between the components. This corresponds to a phase shift of 0.1 degrees for a 10 Hz wave and proportionally less at lower frequencies, which is considered negligible.

Usually, there are also four single probe signals available at 5 samples/s. As only one pair of signals can be simultaneously sampled, two of these signals will have the 28 μs delay (or, in rare instances, 56 μs) with respect to the other two. This delay, corresponding 0.02 degrees (or, in some rare cases, 0.04 degrees) phase shift, is negligible and no information is provided to compensate for it.

2.4.3 Time stamps of EFW data at 450 samples/s

The EFW data obtained at 450 samples/s (Section 2.2), can usually be used without any correction of the time stamps.

The two symmetric E-field components in the spinning reference frame (formed from two pairs of opposing EFW probes), p12 and p34, are constructed by analog differentiation before sampling and are therefore exactly synchronized, in contrast to the data at 25 samples/s discussed in section 2.4.2. Thus, the time stamps given apply to all data.

For a spacecraft where one probe has failed, signals from non-orthogonal pairs (e.g. p32 and p34 in the case of a p1 failure) were digitally formed onboard to provide the full 2D electric field. While (in this case) p34 is available as one analog signal, p32 had to be digitally formed from p2 and p3. Therefore, in these cases the signal from the non-symmetric pair lags the signal from the symmetric pair by 28 μs. This corresponds to a phase shift of less than 2 degrees for a wave at 180 Hz and proportionally less at lower frequencies. This can typically be neglected. Note that this slight time shift between probe pairs is present when despinning data to the ISR2 coordinate system (Section 3.3).

3 Instrument Operations and Processing

3.1 Summary of operations

Table 2 gives an overview of the operational status of the EFW probes on the four spacecraft. The user should be aware that the full resolution (Level 2) electric field data are affected by the number of probes available for E-field measurements. On spacecraft with only 2 functional probes the despun electric field will have a large spin variation and is of limited use. With 3 probes the despun electric field will have some spin variation, depending on the plasma environment. The quality indicators for the Level 2 electric field data are set accordingly; see Table 9.

3.2 Measurement calibration and processing

In processing the EFW data for the CAA, the EFW team uses a combination of ground and in-orbit calibrations. The in-orbit calibrations incorporate extensive cross-calibration with other instruments and inter-calibration between the 4 satellites. Further information is contained in the CAA-EFW Calibration Report and Appendix A below.

3.3 Coordinate systems

The EFW instrument measures the electric field only in the spacecraft spin plane. The preferred coordinate system for scientific studies involving the electric field is therefore a spin-plane oriented coordinate system. The **ISR2** (Inverted Spin Reference) system, also known as **DSI** (Despun System Inverted), is such a system. The x-axis is in the spin plane and pointing as near sunward as possible. The y-axis is in the spin plane, perpendicular to the sunward direction, positive towards dusk. The z-axis is along the (negative) spacecraft spin axis, positive towards the north ecliptic. (The coordinate system is called “Inverted” because Cluster is actually “inverted” with the spin axis pointing towards the south ecliptic.)

Table 2. Operational status.

Space-craft	Time period	Number of E-field probes available	Raw E-field signals available	Quality, full-resolution electric field data*
SC1	2001-02-01 – 2001-12-28	4 (p1,p2,p3,p4)	p12 and p34	3
	2001-12-28 – 2003-09-29	2 (p3,p4)	p34 only	1
	2003-09-29 – 2009-04-19	3 (p2,p3,p4)	p32 and p34	2
	2009-04-19 – 2009-05-07	2 (p2,p3)	p32only	1
	2009-05-07 – 2009-10-14	3 (p2,p3,p4)	p32 and p34	2
	2009-10-14 – 2018-12-10	2 (p2,p3)	p32 only	1
	2018-12-10 – 2024-09-30	1 (p2)	none	0
SC2	2001-02-01 – 2007-05-13	4 (p1,p2,p3,p4)	p12 and p34	3
	2007-05-13 – 2007-11-24	2 (p3,p4)	p34 only	2
	2007-11-24 – 2015-10-12	3 (p2,p3,p4)	p32 and p34	2
	2015-10-12 – 2022-08-23	2 (p3,p4)	p34 only	1
	2022-08-23 – 2024-09-30	1 (p4)	none	0
SC3	2001-02-01 – 2002-07-29	4 (p1,p2,p3,p4)	p12 and p34	3
	2002-07-29 – 2003-09-29	2 (p3,p4)	p34 only	1
	2003-09-29 – 2011-06-01	3 (p2,p3,p4)	p32 and p34	2
	2011-06-01 – 2014-11-03	2 (p2,p4)	none	0
	2014-11-03 – 2024-04-28	1 (p4)	none	0
	2024-04-28 – 2024-09-30	0	none	0
SC4	2001-02-01 – 2013-07-01	4 (p1,p2,p3,p4)	p12 and p34	3
	2013-07-01 – 2015-02-17	3 (p1,p2,p3)	p12 only	1
	2015-02-17 – 2024-09-30	2 (p1,p2)	p12 only	1

* the quality can be reduced from these values during non-favourable plasma conditions for the double probe measurements. On the other hand in some conditions the quality of data may be better than the given quality value may suggest (see Table 9).

The difference between **ISR2** (**DSI**) and **GSE** (Geocentric Solar Ecliptic) is primarily a rotation of between 2 and 7 degrees around the y-axis, which is due to the fact that the spacecraft is slightly tilted so as not to shadow the EFW probes. In the intervals between attitude adjustments on the spacecraft, a very small rotation can also be present about the x-axis.

***Note*: The ISR2 and GSE systems differ substantially on C3 during the May 2008 "tilt campaign" (between 09:00 UT on 2008-04-25 and 08:24 UT on 2008-05-30), when the spin axis of C3 was deliberately tilted by up to 45 degrees about the x-axis.**

4 EFW Science Datasets

4.1 Raw data

Full resolution nominal science raw data are stored as CAA products **L1_P** (spacecraft potential) and **L1_E** (potential differences between probes). These products supersede the earlier products **L1_P1, L1_P2, L1_P3, L1_P4, L1_P12, L1_P34** and **L1_P32**. These Level 1 (L1) products contain datasets that may be useful to the user interested in minimally-processed data, but are not intended for the general science user. (For details of these products, see the CAA Interface Control Document for EFW.)

The production procedures for L1 data involves only decommutation and calibration into physical units. The sun reference pulse data necessary to fully interpret these data are available in the Spin Timing dataset (a CAA auxiliary dataset). The sun sensor is located between probes p2 and p3, 63.8 degrees from the +ZSAT axis (see Figure 1). Selected housekeeping data are available as the L2_HK product at 32 sec resolution.

Note that L1_E (and L2_E) are not available from Cluster 3 during the period 2011-06-01 to 2014-11-03 in spite of the fact that two probes are operational, Table 2. These products are usually calculated onboard, but not for this time period. Here L3_E is calculated using data from individual probes, available from L1_P. After 2014-11-03 only one probe is operational and the electric field is not available.

In addition to nominal science raw data, there are very short intervals of high-resolution EFW internal burst data, see section 4.6 .

4.2 Choosing which data set to use

This and the following sections are included to help users select the appropriate data product. Essentially, the choice boils down to 2 or 3 questions:

1. Are you interested in spacecraft potential measurements, electric field measurements, E × B drift velocities or something else (non-science)?
2. What measurement cadence do you want (full resolution or 4 second resolution)?
3. For electric field measurements, what frame do you want?

The answer to the first question should be obvious. The second and third questions, on the other hand, may be more subtle than they look. When selecting the cadence, keep in mind that the spin period of the spacecraft is roughly 4 seconds, and we take care to do the averaging in such a way as to always take any detected errors into consideration when we process the 4 second resolution data. In general, **unless you really need resolution better than 4 seconds, the EFW team always recommends the 4-second resolution data.** The period of exactly 4 seconds was chosen rather than locking the timing to the spin period in order to make longer-duration spectral studies possible. Answering this question will tell you whether you need L2 (full resolution from despinning) or L3 (4-second resolution from least-squares fitting) datasets.

The user must always keep in mind that **EFW only measures 2 components of the electric field**, and also that the sunward component has a larger DC measurement uncertainty. Rotation

away from the measurement frame (e.g. rotation to GSE) is inherently a 3D operation, and may therefore introduce systematic errors. The natural coordinate system for EFW data is the ISR2 data system. This is discussed in more detail in Section 3.3 . Data in GSE coordinates should be used only if truly required for the analysis.

***Note*: The EFW team recommends the ISR2 frame for most analysis.**

4.3 Science data: spacecraft potential

The science datasets for the spacecraft potential are listed in Table 3. See Section 5.1 for recommendations and caveats regarding spacecraft potential measurements.

Table 3. Science data: spacecraft potential

Sampling rate	CAA Dataset name	Description
5 s^{-1}	L2_P	Spacecraft potential (0.2 sec resolution)
0.25 s^{-1}	L3_P	Spacecraft potential (4 sec resolution)

L2_P and **L3_P** are normally the average potential of all available probes, measured relative to the spacecraft. If all four probes are available, the average is done over all 4 probes. If only two or three probes are available, the average is done over 2 opposing probes (**P1** and **P2**, or **P3** and **P4**). If only two non-opposing probes are available (e.g. **P2** and **P3**), this quantity is the value of one of the probes. If only one probe is available, this quantity is the value of that probe. The probes used are given by the parameter P_probes. When moderate high-bias saturation is detected on one of the probes (indicated by bit 14 in the P_bitmask), the average over 4 seconds in L3_P is replaced by the maximum value (see Section 5.1.5); also the data quality is lowered for such intervals. The individual probe potentials are available in the ancillary data.

4.4 Science data: electric field

The science datasets for the electric field are listed in Table 4. All electric field datasets include quality indicators (see Section 6). For help on choosing an appropriate frame, see Section 3.3. The sampling rate of the electric field measurements can vary in the full-resolution datasets depending on the spacecraft telemetry mode; to find the spacecraft telemetry mode, see CAA Auxiliary (Dataset name: “Telemetry Mode” or C[n]_CT_AUX_TMMODE).

***Note*: Check the quality indicators before using any electric field data product.**

Table 4. Science data: electric field			
Sampling rate	**Frame**	**CAA Dataset name**	**Dataset title**
0.25 s^{-1}	ISR2	L3_E	2D Electric field, (4 sec resolution)
	ISR2, inertial	L3_E3D_INERT	3D Electric field in ISR2 (E·B=0) (4 sec resolution)
	GSE, inertial	L3_E3D_GSE	3D Electric field in GSE (E·B=0) (4 sec resolution)
25 s^{-1} or 450 s^{-1}	ISR2	L2_E	2D Electric field (full resolution)
	ISR2, inertial	L2_E3D_INERT	3D Electric field in ISR2 (E·B=0) (full resolution)
	GSE, inertial	L2_E3D_GSE	3D Electric field in GSE (E·B=0) (full resolution)

L3_E is the 2D electric field vector (E_x and E_y) in the spin plane, computed from a least-squares fit of a sine wave to one probe pair (**P12** or **P34**) over 4 seconds (approximately one spin). The least-squares fit is normally done on **P34**, if available, otherwise on **P12**. The result is two components of the electric field (E_x and E_y) and a measure of the standard deviation of the raw data points from a sine wave (sigma - proxy for wave power at higher frequencies). Also included in this dataset are quality indicators E_quality and E_bitmask (see Section 6). This data is in the ISR2 (instrument) coordinate system (see Section 3.3) and forms the basis from which the L3 science datasets are calculated.

L3_E3D_INERT is the 3D electric field vector in the spin plane in the inertial reference frame. It is computed from **L3_E** by first subtracting the spacecraft motion-induced electric field $\mathbf{v_{sc}} \times \mathbf{B}$, and then computing the third (non-measured axial) component of the electric field using the assumption $\mathbf{E}\cdot\mathbf{B} = 0$. These computations are done at the CAA using the CAA FGM 5VPS dataset. The third component is only computed when the magnetic field direction is more than 15 degrees away from the spin plane and $|\mathbf{B_Z}|$ is larger than 2 nT (otherwise the error in the third electric field component becomes too large). If these requirements are not met, then fill values are inserted in the third component. An error estimate for the third component is also provided. If using the third component, one should always keep in mind that it is artificially constructed and not actually measured.

***Note*: L3_E3D_INERT is the preferred data product for most analyses.**

L3_E3D_GSE is the 3D electric field vector in the GSE coordinate system. It is computed from L3_E3D_INERT by rotating from the ISR2 coordinate system to the GSE system. This rotation mixes together the two measured components with the third (unmeasured) component. This product is only available when the third component can be constructed, and may therefore contain long intervals of fill values when the magnetic field is near the spin plane or when $|\mathbf{B_Z}|$

becomes small. Since the assumption **E**·**B** = 0 is used in the creation of this dataset, the GSE electric field is perpendicular to **B** by construction.

L2_E is the 2D electric field vector (E_x and E_y) in the spin plane and in the spacecraft reference frame, computed using as many probes as are available. It is in the ISR2 (instrument) coordinate system (see Section 3.3) and is the basis from which the other L2 data sets are calculated. One should note that L2_E as well as L2_E3D_INERT (only E_x and E_y) are the only datasets where one could possibly detect parallel electric fields and this is possible only when the magnetic field is close (within several degrees) to the spacecraft spin plane.

L2_E3D_INERT is computed from L2_E in the same manner as L3_E3D_INERT is computed from L3_E (see above). **L2_E3D_INERT is the preferred data product for analyses requiring full-resolution data.** If using the third component, one should additionally be aware that the assumption **E**·**B** = 0 may not be valid at higher frequencies.

L2_E3D_GSE is computed from L2_E3D_INERT in the same manner as L3_E3D_GSE is computed from L3_E3D_INERT (see above). In addition to the problems listed above under L3_E3D_GSE, the assumption **E.B** = 0 may not be valid at higher frequencies. Users are encouraged to consider the other electric field datasets if at all possible.

4.5 Science data: E×B drift velocities

The science datasets for the E×B drifts are listed in Table 5. These datasets contain the plasma convection flow velocity, computed from the 3D electric field vector E (E3D_INERT) and the magnetic field vector **B** as **V** = (**E** × **B**) / $\mathbf{B}^2$. The 4-second averages of the CAA FGM 5VPS dataset has been used here for 4-second datasets and the FGM full-resolution dataset (interpolated to the EFW time stamps) for full-resolution drift velocity datasets. All drift datasets include quality indicators derived from the underlying electric field data (see Section 6). **Users must check the quality indicators E_quality and/or E_bitmask before using any E×B data product**. The drift velocity is given in two frames, ISR2 and GSE.

Table 5. Science data: E×B drift velocities

Sampling rate	Frame	CAA Dataset name	Description
25 s^{-1} or 450 s^{-1}	ISR2	L2_V3D_INERT	E×B drift velocity in ISR2 (full resolution)
	GSE	L2_V3D_GSE	E×B drift velocity in GSE (full resolution)
0.25 s^{-1}	ISR2	L3_V3D_INERT	E×B drift velocity in ISR2 (4 sec resolution)
	GSE	L3_V3D_GSE	E×B drift velocity in GSE (4 sec resolution)

Computing the drift velocity in any frame inherently requires the assumption **E·B = 0** to construct the unmeasured third (axial) component of E. This computation in turn requires that **B** is more than 15 degrees away from the spin plane and that **|B|** > 2 nT (see Section 4.4). If these requirements are not met, then the drift velocity data will contain fill values except the z component in ISR2 that can be calculated from the measured x and y components of the electric field.

Note: **All convection velocities are given in an inertial frame (i.e. with the spacecraft velocity subtracted).**

4.6 Science data: EFW internal burst

The EFW internal bursts are typically very short (several tens of seconds) intervals of high-resolution data. There are typically two bursts per orbit, the collection of which was triggered by an onboard trigger. The science datasets for the EFW internal burst are listed in Table 6.

Table 6. Science data: EFW internal burst

Sampling rate	CAA Dataset name	Description
450 to 18,000 s^{-1}	L2_PB	Spacecraft potential
450 to 18,000 s^{-1}	L2_EB	2D electric field in ISR2 coordinates, spacecraft reference frame
450 to 18,000 s^{-1}	L2_BB	3D magnetic field ISR2 coordinates

Availability of data for a particular burst depends on the signals which were sampled. **L2_EB** is the dataset equivalent to **L2_E** (see Section 4.4). **L2_PB** is computed in a similar manner as the **L2_P** (see Section 4.3). **L2_PB** is not always available, as it requires at least one measurement of the probe-to-spacecraft potential. **L2_BB** is based on the magnetic signals from STAFF-SC sensors and is available for a relatively small fraction of the bursts. When **L2_BB** is available, also **L2_EB** is often available, but for technical reasons sometimes this latter parameter could not be obtained.

4.7 Ancillary data

The CAA contains some additional ancillary datasets that may be useful to the user interested in minimally-processed or historical data. These data are not intended for the general user. Note that **L1_P** (spacecraft potential) and **L1_E** (potential differences between probes) supersede the earlier products **L1_P1, L1_P2, L1_P3, L1_P4, L1_P12, L1_P34** and **L1_P32.** These earlier products are discussed below for completeness. (For details of all these products, see the CAA Interface Control Document for EFW.)

Table 7. Ancillary data		
Sampling rate	**CAA Dataset name**	**Description**
5 s^{-1}	C[n]_CP_EFW_L1_P	Potential, Probe 1, 2, 3, 4 to spacecraft
25 s^{-1} or 450 s^{-1}	C[n]_CP_EFW_L1_E	Potential differences between probes, flag indicating probes 32 or 12
5 s^{-1}	C[n]_CP_EFW_L1_P1	Potential, Probe 1 to spacecraft
	C[n]_CP_EFW_L1_P2	Potential, Probe 2 to spacecraft
	C[n]_CP_EFW_L1_P3	Potential, Probe 3 to spacecraft
	C[n]_CP_EFW_L1_P4	Potential, Probe 4 to spacecraft
25 s^{-1} or 450 s^{-1}	C[n]_CP_EFW_L1_P12	Potential, Probe 1 to Probe 2
	C[n]_CP_EFW_L1_P32	Potential, Probe 3 to Probe 2
	C[n]_CP_EFW_L1_P34	Potential, Probe 3 to Probe 4
450 to 18.000 s^{-1}	C[n]_CP_EFW_L1_IB	Up to 8 parameters collected during the EFW internal burst
0.25 s^{-1}	C[n]_CP_EFW_L3_DER	Electric Field offsets (4 second resolution)
0.25 s^{-1}	C[n]_CP_EFW_L3_SFIT	Spinfits of the electric field from the individual probe pairs
0.25 s^{-1}	C[n]_PP_EFW	Preliminary Electric Field parameters (4 second resolution)
1/32 s^{-1}	C[n]_CP_EFW_L2_HK	Instrument settings
1/60 s^{-1}	SP_EFW	Preliminary Electric Field parameters (one spacecraft, 1 minute resolution)

Table 7. EFW data products in the CAA. For details of PP_EFW and SP_EFW see the Users Guide to the Cluster Science Data System, and for all other products see the CAA Interface Control Document for EFW.

The Level 1 datasets (L1) are the ***raw data*** from the instrument, decommutated and converted to physical units (except for the internal burst which is provided in TM units). The dataset **P** includes the potentials of the four individual probes, measured relative to the spacecraft. The dataset **E** includes the electric field in the satellite spin plane. The obsolete datasets **P1**, **P2**, **P3**, **P4** are the potentials of the four individual probes, measured relative to the spacecraft and the obsolete datasets **P12**, **P34** and **P32** are potential differences between pairs of probes.

C[n]_CP_EFW_L3_DER is the DC offset in the raw data. See Appendix A.1. for more information. **DER** is a vector with 2 components corresponding to either the offsets in p12 and p34 or the offsets in p32 and p34.

C[n]_PP_EFW and **SP_EFW** are preliminary data from the CSDS system. They are included mostly for historical purposes.

5 Recommendations and caveats

Much effort has been spent on calibrating the data and removing spurious effects to give a useful database for scientific analysis. In spite of this, there will be data in the CAA which are not of optimum quality. It is important that anyone using the EFW CAA data be aware of the pertinent measurement issues to avoid misinterpretations of the data.

5.1 Spacecraft potential

There are point-by-point quality flags and bitmasks attached to the spacecraft potential data, as there is for the electric field data (see Section 6). This section therefore describes some of the problems of which the user should be aware and which are not necessarily indicated by the bitmask.

5.1.1 Spacecraft-to-plasma potential

The "spacecraft potential" in the CAA-EFW data products reflects the potential of the biased probes with respect to the spacecraft. This is not exactly the same as the potential of the spacecraft with respect to the plasma. First of all, note the sign convention: the Cluster spacecraft are usually positive with respect to the plasma, so the probe-to-spacecraft potential data in the CAA is typically negative. Second, the probes typically also float somewhat positive with respect to the plasma, but at a very much smaller potential than the satellite (roughly 1 V, as compared to up to over 70 V for the spacecraft). Third, the probes are affected by the potential on the long wire booms, and hence the true spacecraft-to-plasma potential may be somewhat larger (up to 23% in tenuous plasmas). Users who require the spacecraft-to-plasma potential are referred to Cully et al. [2007], Pedersen et al. [2008] and André et al. [2015].

5.1.2 ASPOC operations

The ASPOC instrument attempts to keep the spacecraft potential at a low value, primarily to enable low-energy ion and electron measurements by the particle instruments. In the absence of ASPOC the spacecraft potential often reaches several tens of volts in the low-density plasmas encountered by Cluster. With ASPOC operating, the spacecraft potential is brought down to the order of 5-8 V. A positive side-effect of this is that the electric field measurements are most often improved since the wake effects associated with large spacecraft potentials in the polar cap (see Section 6.12) are drastically reduced.

The spacecraft potential is often used as a proxy for ambient plasma density variations [see Pedersen et al., 2008]. Any use of the spacecraft potential to determine plasma density should take into account whether ASPOC was operating or not, which is indicated by the ASPOC_status parameter included with L2/3_P. ASPOC was never operational on Cluster 1. Due to the end of Indium ions, ASPOC was in general not operated after 2006 on the other spacecraft.

5.1.3 EDI operations

EDI measures the ambient electric field by emitting a beam of electrons and detecting the drift step as the electrons gyrate around the ambient magnetic field. The emitted beam current contributes to increasing the spacecraft potential, and the effects can be particularly large in a low density plasma. During some periods in the beginning of the mission, the emitted EDI beam current was larger than expected, in particular on Cluster 2, so there is a tendency for the spacecraft potential to be larger than on the other spacecraft. Since the spacecraft potential is often used as a proxy for a measurement of the ambient plasma density, this could be misinterpreted as a lower density at Cluster 2. This problem was alleviated on 8 April 2004, when the EDI guns on C2 were turned off in favour of running the instrument in an alternative "ambient" mode.

Normal EDI operations also affect the potential somewhat, especially when run in the high beam current mode. In later years (after about 2004), the potentials on C1 and C3 (where EDI is run) are often notably different from the potentials on C2 and C4 in the same plasma environment. Note that EDI was never operational on C4.

5.1.4 WHISPER operations

The WHISPER instrument regularly emits waves using the EFW probes to detect resonance frequencies in the ambient plasma. The WHISPER active soundings are done regularly, often at a repetition period of 52 s or 104 s, so they should be easy to separate from real variations in the data. The soundings are also marked in the EFW spacecraft potential and electric field data (bit 13 in the P_bitmaskA , also see Section 6.14). The spacecraft potential is set to fill values at the times of soundings.

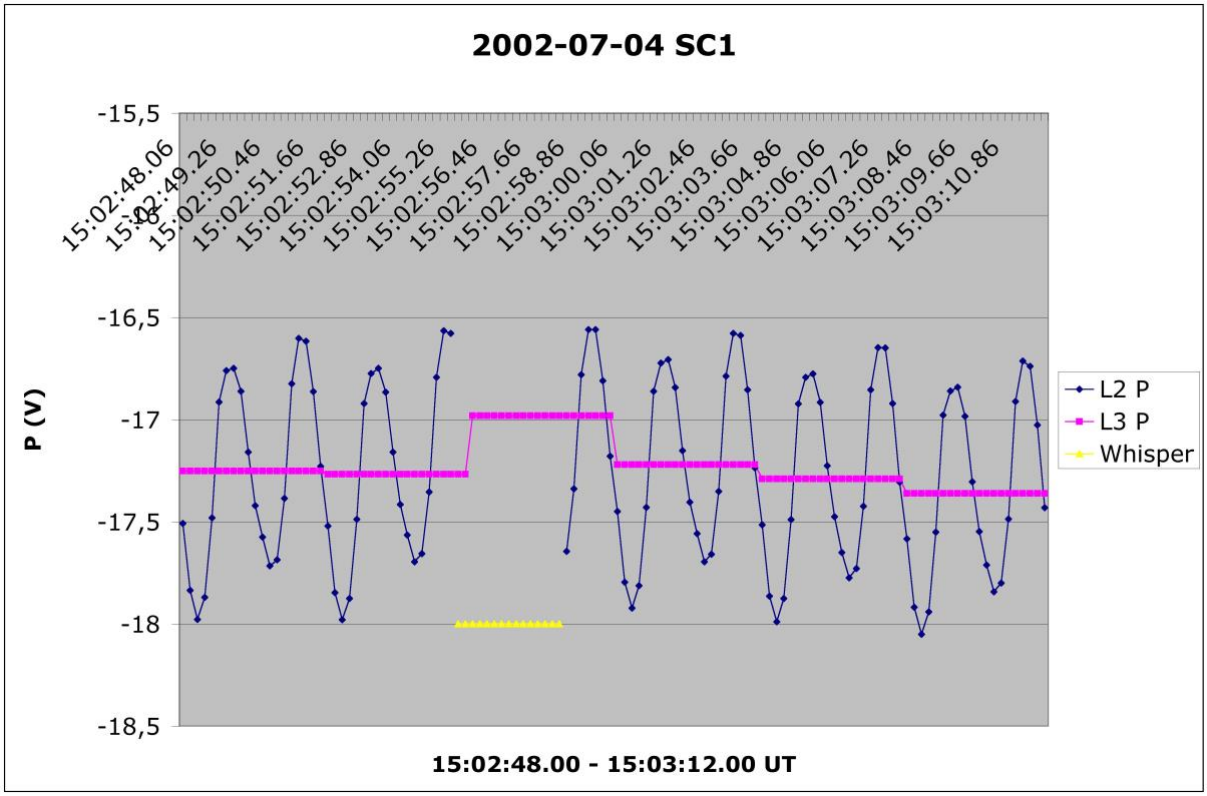

Figure 3: Peak in the L3_P (4-sec resolution) introduced by averaging over a time interval containing a data gap caused by the WHISPER active sounding.

The spacecraft potential is normally computed from an average of the potential of opposing probes (4 or 2) in the electric field mode, i.e., biased with a negative current to compensate for photoemission and keep the probes near plasma potential. L2_P has a time resolution of 5 s^{-1}, the same as the raw data, and varies up and down as the spacecraft spins. The L3 quantity is a 4-second average of L2_P where the spin variation is essentially eliminated.

Due to the removal of raw data when the WHISPER instrument is in its active sounding mode, there will be gaps in L2_P (and sometimes also in L3_P). Since the WHISPER soundings are not synchronized to the spin, the gaps in L2_P may occur at any spin phase, and L3_P computed near such a gap may have contributions from different parts of the spin depending on the exact timing of individual samples relative to the spin. This has the end effect that L3_P may have small peaks or drops which are related to the WHISPER active duty cycle, illustrated in Figure 3.

5.1.5 High bias saturation

The EFW instruments draw a bias current from the plasma in order to anchor the probes to the local plasma potential. If this bias current is too large, then the probes behave extremely non-linearly and shoot to large negative potentials ("saturate"). This happens on occasion when the plasma density is high. Moderate saturation results in spikes in the potential whenever the affected probe points sunward, while full saturation sends the probes to their minimum value

of -68 volts. As an example, the problem was worse in 2005 and early 2006, and was largely eliminated by a change in the bias settings on 16 June 2006. See also the CAA-EFW Calibration Report.

The processing software automatically detects high bias saturation intervals on a probe-by-probe basis. The affected intervals are indicated by bit 14 in the P_bitmask. When a problem with high bias saturation is detected, data from severely affected probes (those that reach -68 volts) is first discarded, and then the L2 and L3 data are computed from the maximum potential of the remaining operational probes. By using the maximum value instead of the mean value, the data is only slightly affected when one probe spikes toward large negative values. Since only one probe at a time can point in the sunward direction, the resulting timeseries does not exhibit the large spikes in the underlying signals.

Spin variations in the spacecraft potential are a real and expected effect resulting from the changing photoemissive area of the spacecraft. However, large (> 5V) spin-synchronous spikes in L2_P in a high density environment (L3_P > -10 V) should be treated as suspicious. Check whether high bias saturation was detected by checking bit 14 of E_bitmask for electric field data during the interval.

5.1.6 Comparison between spacecraft

The Cluster satellites are identical in design. In consequence, two Cluster spacecraft should ideally acquire the same spacecraft potential if subject to the same plasma conditions, assuming onboard systems capable of influencing the spacecraft potential are operated identically. There are exceptions to this last assumption already early on in the mission, but the operational differences have increased with age during the mission. In addition to ASPOC (Section 5.1.2) and EDI (Section 5.1.3), the operations of EFW itself impacts the spacecraft potential. At the start of the mission, all 16 (4x4) EFW probes were operational, with identical settings for bias currents and guard/puck voltages on each spacecraft. A probe may fail (Section 2.2) in various ways, but whatever the failure mode the probe (and its adjacent biased elements) usually ends up at a different potential with respect to the plasma, impacting the total current balance of the spacecraft and hence its potential. Even if in identical plasma conditions, the potential of two spacecraft therefore is different from the time a probe fails on one of them. The effect is strongest in tenuous plasmas, where the total current emitted by biased EFW is a larger contribution to the spacecraft current balance and hardly noticeable in dense plasmas (Figure 4). When settings of probe, guard and stub voltages on the failed probe are changed to minimize the impact of the failure on WEC measurements the relation of the spacecraft potential to plasma parameters might again change. As a result of these and other differences between spacecraft, if the EFW probe to spacecraft potential is seen to be different on two spacecraft, this cannot immediately be interpreted as due to different plasma conditions at their positions.

It should be noted that these issues impact the spacecraft potential as such, not the quality of the probe to spacecraft potential as a measure of it. The archived spacecraft potential data is still a good measure of (the negative of) the potential of any spacecraft at any given time

.

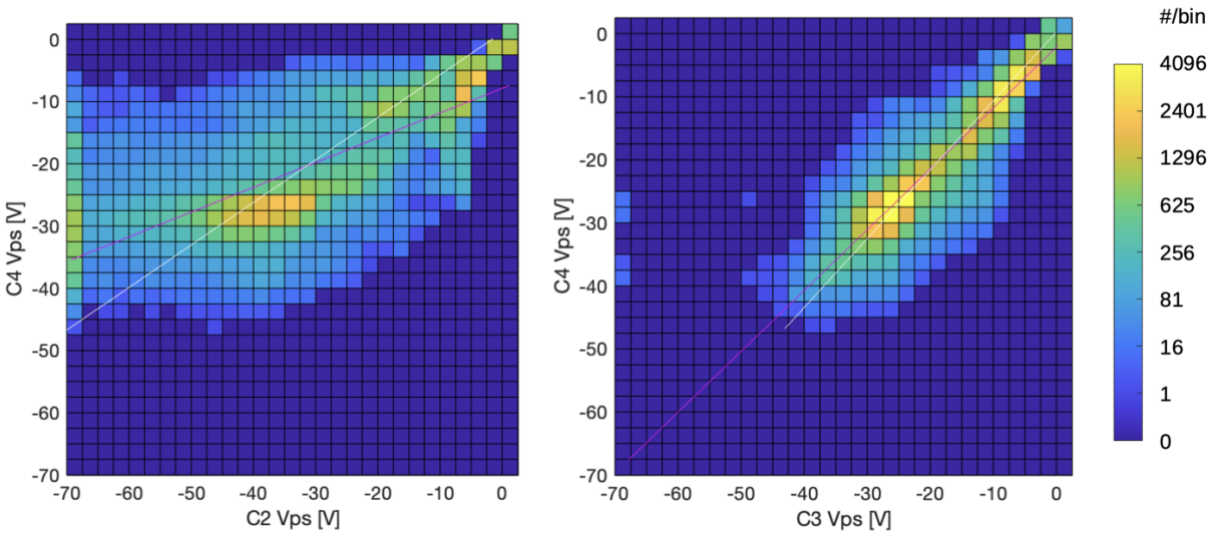

Figure 4. Statistics of simultaneous probe to spacecraft potential measurements on some Cluster spacecraft during 100 hours in the magnetotail in 2022 (four representative tail lobe crossings from Aug 29 to Sep 6, in total 89,136 data points at 4s time resolution, histogram bin size 2.5x2.5V). Cluster 3 and Cluster 4 can be seen to follow each other closely, with variations as expected by natural differences over the separation distance. An EFW probe on Cluster 2 is stuck at -70V during this interval. This probe and its puck and guard therefore emits more photoelectrons than other probes, driving C2 to higher positive spacecraft potential. The probe to spacecraft potential on C2 (measured by another, non-stuck, EFW probe) therefore is more negative than on C4. Part of the higher spread in the left plot is due to longer distance between C2-C4 than C3-C4.

5.1.7 Estimate of the plasma density

The spacecraft potential depends on the plasma density. After calibration using other Cluster instruments, the potential delivered by EFW often can be used to estimate the total density (Pedersen et al., 2008; Lybekk et al. 2012; André et al., 2015; Roberts et al., 2020). Since estimates of the potential can vary between spacecraft (Section 5.1.6), individual calibration for each spacecraft should be used. Furthermore, changes in solar EUV radiation as well as differences in operational settings will change the calibration with time. An overview of some operational settings is given in Appendix B. Effects mentioned in previous sections, including ASPOC, WHISPER and EDI operations, and high bias saturation, will affect the spacecraft potential. During such conditions calibrations obtained during quiet routine operations should not be used. Density estimates can still sometimes be attempted (Andriopoulous et al, 2015).

5.2 Electric field data

All EFW data in the CAA has a quality parameter attached to it, which is described in Section 6 ; this section describes other general caveats that are not specifically flagged.

***Note*: Users must check the quality parameter before using the data.**

5.2.1 Instrument noise level

The EFW electronics are optimized primarily for lower frequencies and larger amplitudes. However, some users may be interested in very weak AC signals, for example for turbulence studies. For such applications, the user should be aware of the AC instrument noise, which may become visible in the 450 Hz data.

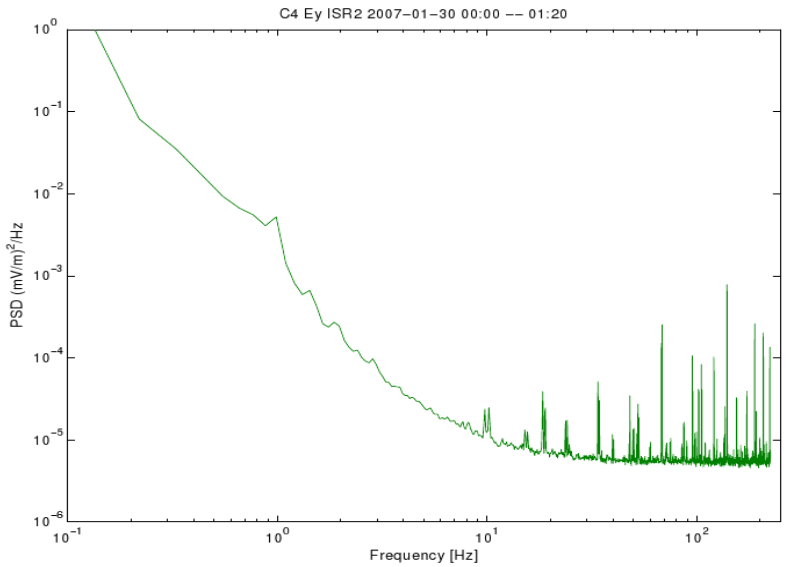

Figure 5: Noise floor as seen in the 450 Hz data.

Figure 5 shows an example of data which reaches the AC noise floor. The noise above a few tens of Hz is set by interference from nearby digital electronics, which causes fluctuations in the electrical ground level. At higher frequencies, there is a roughly white component, plus some discrete lines. The exact spectral density may vary slightly from event to event. The EFW noise is discussed in more detail in the CAA-EFW Calibration Report.

5.2.2 Sunward (ISR2) offsets

Double-probe electric field experiments like EFW are affected by offsets in the sunward direction, caused by asymmetries in the photoelectron emission. The electric field data in the CAA has been corrected for this effect by cross-calibrating the measured electric fields with other instruments, and then subtracting a DC sunward offset, as discussed in Appendix A.2. (see

also the CAA-EFW Calibration Report). However, some offset may still be present in the data even after correction, as the correction relies on an average offset based on a large amount of data, which does not describe short time-scale changes in the offsets.

***Note*: Although relative deviations of a few mV/m can usually be trusted, the uncertainty in the DC offset limits the absolute DC accuracy to roughly 1 mV/m.**

The offset is, however, somewhat dependent on the ambient plasma parameters. We therefore use different offsets in the *solar wind and magnetosheath* (dense plasmas) as compared to the *magnetosphere*. These offsets may differ by a few tenths of a mV/m. Furthermore, the offsets in the solar wind are affected by the solar wind parameters: the sunward offsets are smaller in the high-speed solar wind (not corrected in the CAA). The *magnetosheath* offsets are applied when the negative of the spacecraft potential is above -8 V (e.g. in the inner magnetosphere where it is often only a few volts negative), otherwise the *magnetospheric* set of offsets is used.

The change of offsets is illustrated in Figure 6, which shows that *Ex* changes abruptly several times during a three hour interval because the spacecraft potential is crossing the -8 V level several times. In such cases it is recommended that the users remove the applied ISR2 offsets and deduce the actual ISR2 offsets from comparison to other instruments (EDI, CIS, PEACE). The information about the offsets applied to the electric field data is presented in the FILE_CAVEATS section of a CEF file. Below is an example for the time interval presented in Figure 6: the entry in blue is the offsets in the beginning of the time interval, and the following changes in the offsets (marked by A-D in Figure 6) are in red:

```
START_META    = FILE_CAVEATS
   ENTRY     = "CAA Merged File - $Id: cefmerge.c,v 1.27 2009/04/09
09:40:06 cperry Exp cperry $"
   ENTRY     = "The file caveats for each segment follows:-"
   ENTRY     = "2003-08-08T10:00:00Z/2003-08-08T13:00:00Z ,
C4_CP_EFW_L3_E__20030808_V01"
   ENTRY     = "  2003-08-08T09:00:00.000Z/2003-08-08T10:30:00.000Z
Probe pair p34"
   ENTRY     = "  2003-08-08T09:00:00.000Z/2003-08-08T10:30:00.000Z
ISR2 offsets: dEx=1.43 dEy=0.00, dAmp=1.10"
   ENTRY     = "  2003-08-08T09:00:00.000Z/2003-08-08T10:30:00.000Z
p34 offset (ISR2): dEx=0.00 dEy=0.00"
   ENTRY     = "  2003-08-08T10:30:00.000Z/2003-08-08T12:00:00.000Z
Probe pair p34"
   ENTRY     = "  2003-08-08T10:30:02.000Z/2003-08-08T11:15:02.000Z
ISR2 offsets: dEx=1.43 dEy=0.00, dAmp=1.10"
   ENTRY     = "  2003-08-08T11:15:02.000Z/2003-08-08T12:00:00.000Z
ISR2 offsets: dEx=0.71 dEy=0.00, dAmp=1.10"
   ENTRY     = "  2003-08-08T10:30:00.000Z/2003-08-08T12:00:00.000Z
p34 offset (ISR2): dEx=0.00 dEy=0.00"
   ENTRY     = "  2003-08-08T12:00:00.000Z/2003-08-08T13:30:00.000Z
Probe pair p34"
   ENTRY     = "  2003-08-08T12:00:02.000Z/2003-08-08T12:10:02.000Z
ISR2 offsets: dEx=0.71 dEy=0.00, dAmp=1.10"
   ENTRY     = "  2003-08-08T12:10:02.000Z/2003-08-08T12:15:02.000Z
```

```
ISR2 offsets: dEx=1.43 dEy=0.00, dAmp=1.10"
   ENTRY    = "  2003-08-08T12:15:02.000Z/2003-08-08T12:20:02.000Z
ISR2 offsets: dEx=0.71 dEy=0.00, dAmp=1.10"
   ENTRY    = "  2003-08-08T12:20:02.000Z/2003-08-08T13:30:00.000Z
ISR2 offsets: dEx=1.43 dEy=0.00, dAmp=1.10"
   ENTRY    = "  2003-08-08T12:00:00.000Z/2003-08-08T13:30:00.000Z
p34 offset (ISR2): dEx=0.00 dEy=0.00"
END_META     = FILE_CAVEATS
```

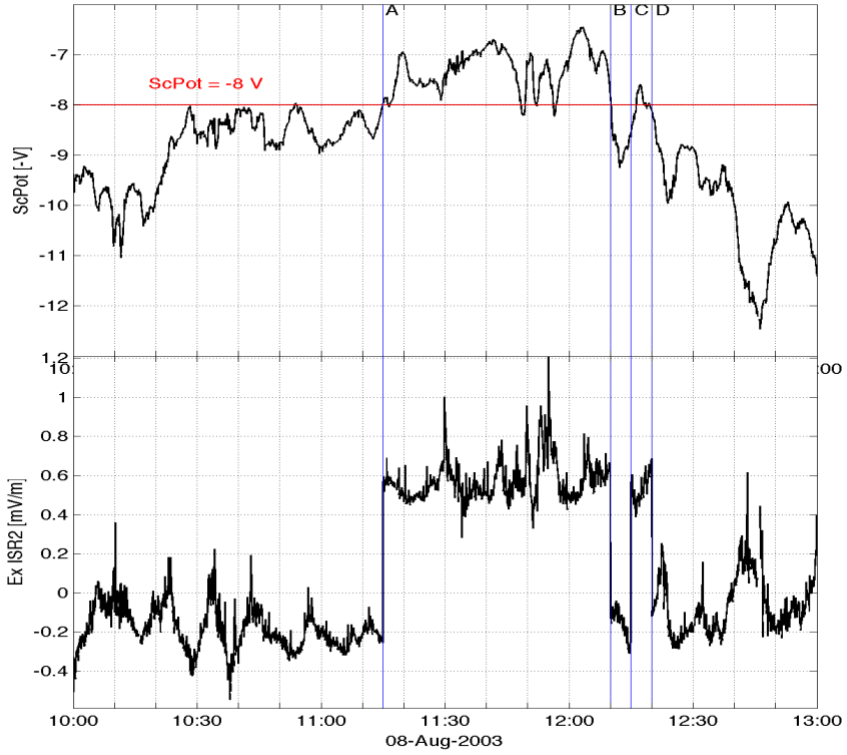

Figure 6: Example showing changing Ex ISR2 offset.

5.3 The commissioning period

The Cluster spacecraft were launched in two pairs on July 16 and August 9, 2000. The orbits were then adjusted and the scientific instruments were switched on, tested and intercalibrated during a 5-month commissioning period. Routine science operations started February 1, 2001.

EFW data from the commissioning period before February 1, 2001, are available in CAA. Data from the period up to and including November 2000 include only Level 1. During this first part of the commissioning, data have been obtained during only a small fraction of the time. Also, the lengths of the wire booms are changing with time as the boom pairs are being deployed in multiple steps on the individual satellites.

EFW data in CAA from the periods December 2000 and January 2001 include Level 1, 2 and 3. During this latter part of the commissioning all wire booms are extended to their full length and data are available during a larger fraction of the time.

Data from the whole commissioning period should be used with care since multiple instruments may be operated in a non-standard way.

Non-standard EFW operations include tests of interference with other instruments and different bias currents to the two probe pairs on one spacecraft. For a list of times for boom deployments during the first part of the commissioning, and for other non-standard operations during the period up to December 4, see http://www.plasma.kth.se/cluster/wec_commiss.html . The various steps A1, A2, …, B1, B2, … are explained in the WEC User Manual, section 5. For a more detailed overview of all the EFW commissioning steps such as boom unit cover opening, boom deployments and spacecraft spin-ups, including plots of the EFW data, please refer to the document "EFW commissioning information", available at the CSA documentation site https://www.cosmos.esa.int/web/csa/documentation, specifically the document https://caa.esac.esa.int/documents/teams/EFW/Cluster_EFW_commissioning_v4.pdf.

6 Quality parameters for the electric field and spacecraft potential data

Each EFW electric field dataset contains the same two record-varying parameters: **E_quality** and **E_bitmask**. For the spacecraft potential these parameters are **P_quality** and **P_bitmask**. These are computed automatically by the processing software and help the user to filter out scientifically poor-quality data values. **E_quality (P_quality)** can be used as a general guide as to whether a given data interval is appropriate for publication, while the **E_bitmask (P_bitmask)** supplies details as to exactly which problems may be present. Users must check these parameters before using any spacecraft potential, electric field or drift velocity data.

Keep in mind that the quality flags are determined automatically. While they are generally quite robust and further verified manually, they are by no means infallible.

E_bitmask (**P_bitmask**) is a binary bit mask indicating various types of problems associated with the data. The meaning of the bits are as follows, and are explained in more detail in the subsections below.

Table 8. Meaning of the E_bitmask and P_bitmask flags

Bit	Decimal value	Meaning	E_quality <=	P_quality <=
0	1	Reset	0	1
1	2	Bad bias	0	1
2	4	Probe saturation	0	1
3	8	Low density saturation (-68V)	0	1
4	16	Sweep (collection and dump)	0	N/A
5	32	Burst dump	0	N/A
6	64	Non-standard operations (NS_OPS)	0	N/A
7	128	Manually set E_quality	N/A	N/A
8	256	Single probe pair (affects only Level 2 data)	1 (L2 only)	N/A
9	512	Asymmetric mode (p32 and p34, affects only Level 2 data)	2 (L2 only)	N/A
10	1024	Solar wind wake correction applied	3	N/A
11	2048	Lobe wake	1	N/A
12	4096	Plasmaspheric wake	1	N/A
13	8192	WHISPER operating	2	0
14	16384	Saturation due to high bias current	1	2 (L3), 1
15	32768	Bias current DAC not responding correctly	2 (L2 only)	N/A
16	65536	Saturation due to probe shadow	1 (L2 only)	2

The resulting value of the bitmask is a binary OR of all the relevant values. For example, if a plasmaspheric wake (bit 12) is detected at the same time as WHISPER is operating (bit 13), then the resulting bitmask is $2^{12}+2^{13}$= 12288. In Matlab this can done using function `bitand()`:

```
>> mask=12288;
>> for bit=0:15, if (bitand(mask, 2^bit)),...
fprintf('Bit #%d set\n',bit), end, end
Bit #12 set
Bit #13 set
>>
```

E_quality (**P_quality**) gives the estimated quality of the electric field (spacecraft potential). Possible values are as follows:

Table 9. E_quality and P_quality definitions

Quality	Meaning
0	Bad data
1	Known problems, use at your own risk
2	Survey data, possibly not publication-quality
3	Good for publication, subject to PI approval
4	Excellent data which has received special treatment

Except in rare circumstances when E_quality is set manually, it is taken as the lowest quality associated with any identified problem. So in the above example with plasmaspheric wake (E_quality<=1) and WHISPER operation (E_quality<=2), E_quality would be 1.

6.1 Reset (bit 0, E_quality=0)

When the EFW instrument is first initialized after an on-orbit reset (usually twice per orbit), it takes up to several hundreds of seconds before the instrument begins operating in the desired mode. Bit 0 of E_bitmask marks any data transmitted before this set-up procedure is complete. These data are generally not useful for any purpose.

6.2 Bad bias (bit 1, E_quality=0)

In order to obtain a reliable measurement of DC fields and spacecraft potential, the EFW instrument draws a bias current from the probes. If this bias current is set incorrectly (for example, because of a commanding error), then bit 1 of E_bitmask is set and E_quality is set to zero. Electric field fluctuations at high frequencies (above a few Hz) may or may not be recoverable from these data, and low-frequency fields should not be trusted. For the latter reasons, the data are kept and delivered to the users.

6.3 Probe latchup (bit 2, E_quality=0)

Occasionally, the EFW probes become stuck at a fixed voltage, independent of the plasma conditions. This is usually the result of a problem in the digital electronics. Under these conditions, we set bit 2 of E_bitmask. These data points are not useful, and we set E_quality to zero. Normally these data have fill values.

6.4 Low density saturation (bit 3, E_quality=0)

The EFW electronics is designed to handle spacecraft potentials up to roughly 68 volts. Beyond this level, the probe potentials saturate and the measured potential differences either become severely distorted (if only one probe saturates) or constant and near-zero (if both probes saturate). No meaningful information about the electric field can be extracted from this data. Normally these data have fill values.

6.5 Sweep data (bit 4, E_quality=0)

Bias current and voltage sweeps are performed at regular intervals (every 2 hours for most of the mission) and usually last for 9 seconds. These sweeps are useful for probe diagnostics for the EFW team. During these sweeps, there is no electric field data. At the moment, the sweep data is not archived in the CAA in any processed form. Normally these data have fill values.

6.6 Burst data (bit 5, E_quality=0)

Internal burst data is collected during short triggered intervals and normally placed into the telemetry once per orbit. When the telemetry stream is interrupted for dumping internal burst data, this is flagged with bit 5 of E_bitmask. The data in the internal burst will have been recorded much earlier than the burst dump.

6.7 Non-standard operations (bit 6, E_quality=0)

Sometimes, problems arise that are outside of normal operations and not covered by the available bits in the bitmask. The EFW team maintains a list of these intervals at:
http://www.cluster.irfu.se/efw/ops/ns_ops.html
This information is also provided as the EFW caveat dataset (ancillary dataset) which is automatically distributed to the users when they request any EFW science dataset. These problems can range from benign to severe. Intervals when the data is adversely affected by these problems are marked with bit 6 of E_bitmask, and E_quality is generally set to zero.

If you see this flag in your data, you should check the list (see link above) or the delivered caveat dataset (CQ_INST) for further details. In some rare circumstances, the data may be useful after careful further processing. Manoeuvres are a frequent reason for flagging non-standard operations, since firing the thrusters creates large plumes of plasma that disturb the measurements. Electric field data acquired during such intervals cannot be corrected.

6.8 Manually-set quality (bit 7)

Each bit in the bitmask is associated with a maximum value for E_quality. However, occasionally, during manual inspection, we encounter intervals when the automatically-determined value of E_quality doesn't agree with the "true" quality of the data, and we set E_quality by hand. These intervals are marked with bit 7 of E_bitmask.

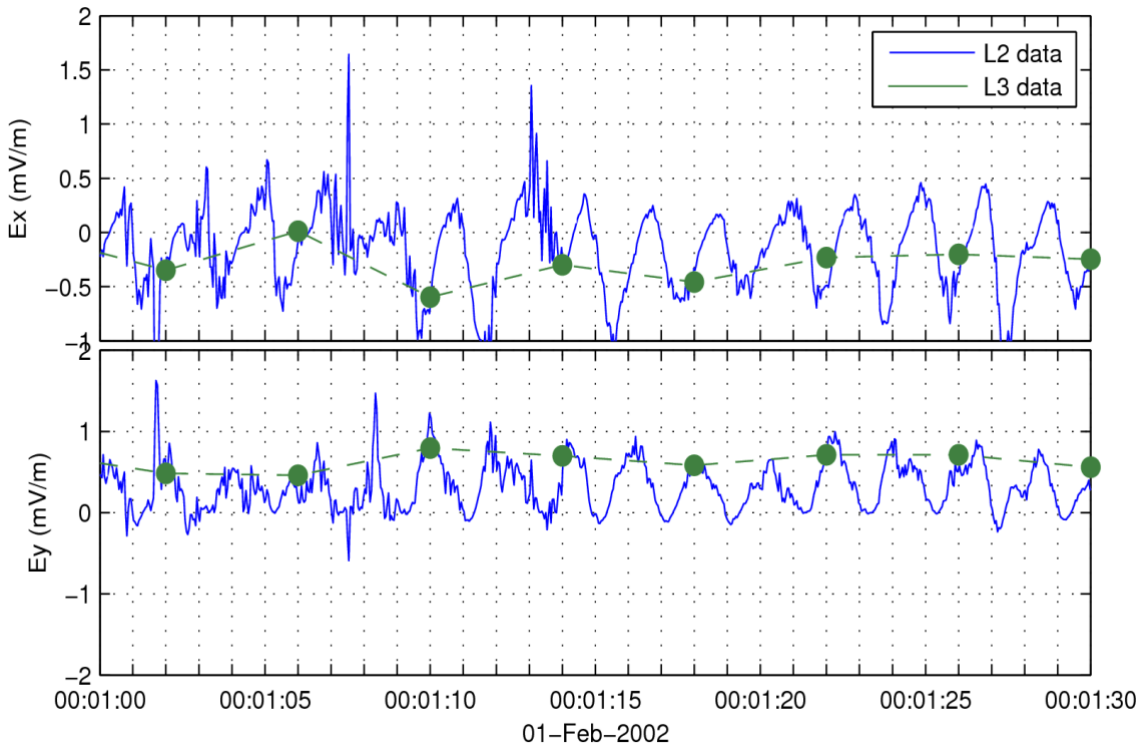

Figure 7: Comparison of L2 (25 s^{-1}, blue) and L3 (4 second resolution, green) for a period when only one probe pair was available.

6.9 Single probe pair (bit 8, E_quality (L2) <=1)

For various reasons, data may be available from one probe pair only. In these intervals, it is impossible to measure the 2D spin-plane electric field faster than at spin resolution.

However, the higher-resolution L2 data may still be of interest to those studying high-frequency waves, and so the L2 data is included in the CAA with E_quality no higher than 1 and bit 8 of E_bitmask set. Prior to despinning, the missing component of E is put to zero. Naturally, the resulting L2 data has a severe spin modulation as seen in Figure 7. The 4 second resolution L3 data relies on one probe pair only and hence is unaffected by the lack of a second probe pair.

6.10 Asymmetric mode (bit 9, E_quality (L2) <=2)

Several of the individual electric field probes have failed (see Section 2.2) As a workaround for this problem, the EFW instrument can be configured to measure voltage differences that do not involve the failed probe. Labelling the voltages at the 4 probes shown in Figure 1 as V1 through V4, the nominal configuration is to measure the longest-baseline orthogonal pairs: (V4-V3) and (V2-V1). If V1 is unavailable due to a hardware failure, then the non-orthogonal pairs (V4-V3) and (V3-V2) are measured instead.

The use of this asymmetric configuration leads to reduced data quality in the L2 data. The 4-second resolution L3 data requires only one probe pair and is hence unaffected. Users interested in L2 data marked as asymmetric mode should be particularly aware of two effects:

- First, the asymmetric data tends to have considerably more spurious power at harmonics of the spin frequency than the symmetric data. Users should always be extremely suspicious of any signals at the spin frequency or its harmonics, and this applies doubly in the asymmetric mode (for more details see the CAA-EFW Calibration Report).
- Second, the solar wind wake cannot be corrected on asymmetric probe pairs. For intervals with one symmetric and one asymmetric pair, the solar wind wake is corrected on the symmetric pair only. This results in a solar wind wake spike once per spin in Ex and once per spin in Ey. The Ex signal sometimes has an additional small lower frequency component, as in Figure 8. These spikes are present in all asymmetric data in the solar wind and are not related to the true geophysical electric field.

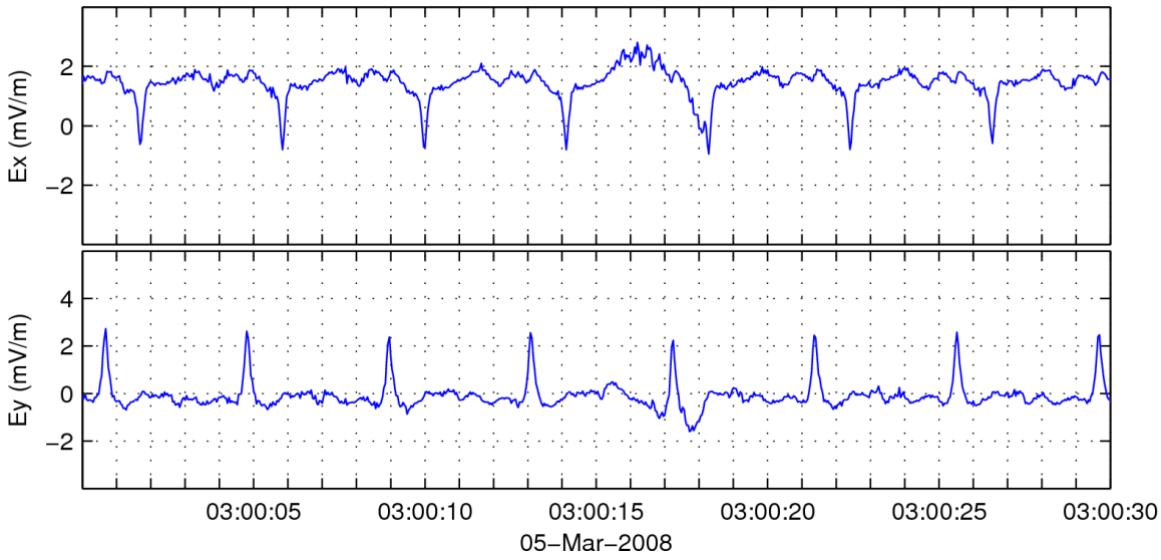

Figure 8: High-resolution (L2) electric field data from C3 when operating in the solar wind in asymmetric mode. Similar spikes in the nominal (symmetric) mode are removed.

6.11 Solar wind wake (bit 10, E_quality unaffected)

The streaming solar wind creates a negatively charged wake behind the spacecraft in the anti-sunward direction. As the individual probes enter and exit this wake, there is a dip in the probe potential, and thus a spike in the raw data signal twice per spin on each probe pair, see the bottom panel in Figure 9. In the de-spun electric field data this shows up as a negative spike in the sunward component Ex, four times per spin, once for each probe entering the wake, which can be clearly seen as a strong signal at 1 Hz and the harmonics in the top panel in Figure 9. An algorithm has been developed to correct for these solar wind wakes in the Level 2 electric field data before submission to the CAA [Eriksson et al., 2007, André et al., 2021].

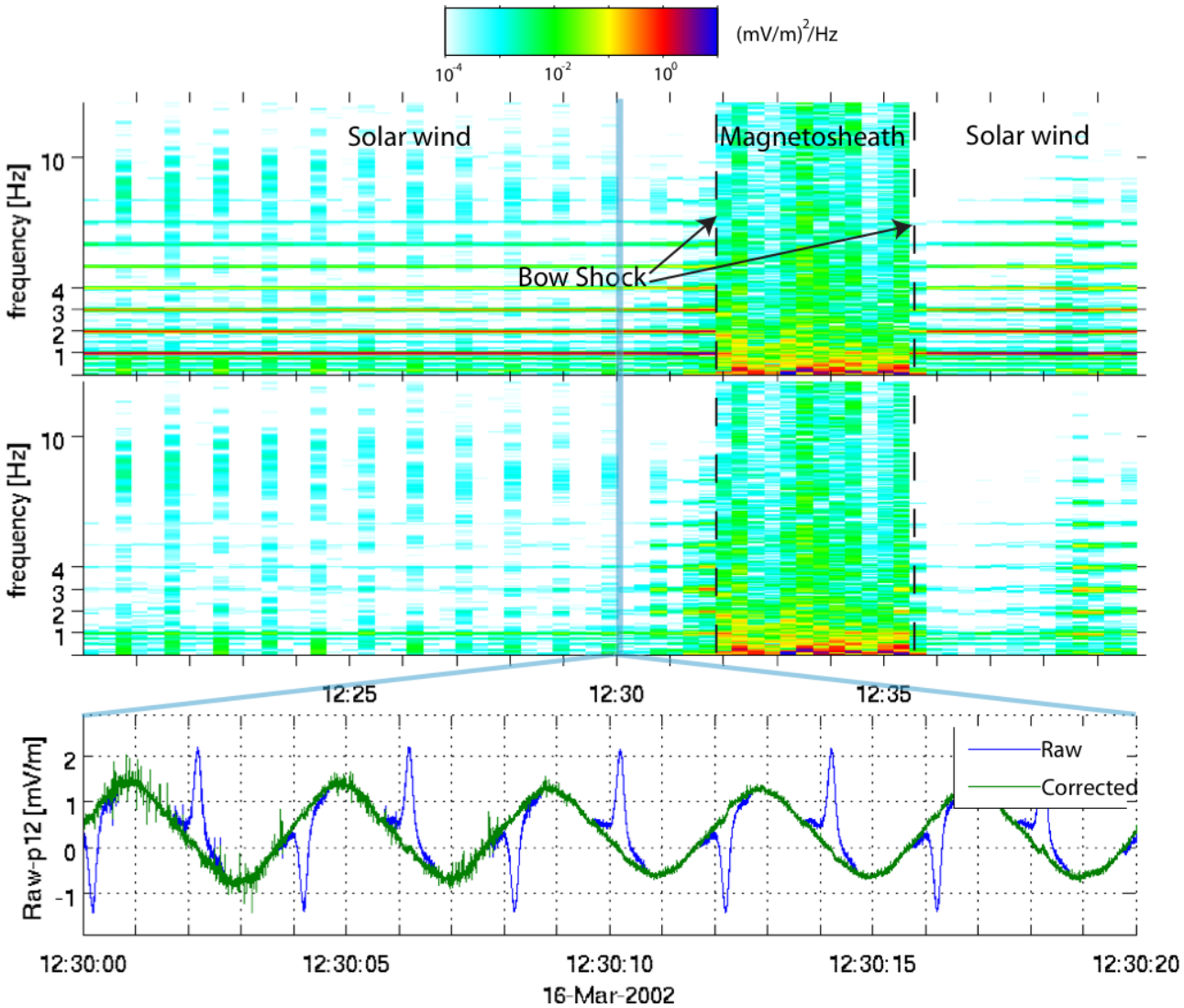

Figure 9: Electric field measurements in the solar wind by Cluster 1. The two upper panels show spectra of Ex ISR2 before and after wake correction. The bottom panel shows raw (blue) and corrected (green) data from p12.

Bit 10 of E_bitmask indicates that this correction has been performed. While generally doing a good job, the algorithm is not always perfect, so the problem with solar wind wakes should be kept in mind as soon as spikes at four times per spin period are encountered in the data. Users should also be wary of any data in which bit 10 toggles on and off throughout the interval, as this may indicate that the processing software missed some wake corrections.

The wake correction procedure is not applied to asymmetric probe pairs (p32), so data collected in asymmetric mode will have spikes twice per spin period (see Section 6.10).

Provided there are no other problems, the corrected data from symmetric pairs is considered fit for publication, and E_quality is not reduced.

6.12 Cold ion drift wake (bit 11, E_quality<=1)

In the low-density plasma encountered in the tail lobes and above the polar caps, there is often a cold plasma component streaming essentially along the magnetic field lines, outward from Earth. This creates a negative wake on the anti-earthward side of the spacecraft, with similar consequences on the data as the solar wind wake (Section 6.11). A difference compared to the solar wind, however, is that the ion drift wake is broader and more diffuse.

It is often very hard to recognize the presence of cold ion drift wakes in the raw data since the effect is similar to that of a real ambient electric field. For an example, see Figure 11 in the CAA-EFW Calibration Report. The CAA production software attempts to detect all such ion wakes by looking at a combination of parameters, such as spacecraft potential, magnetic field direction, and the relation between different electric field components. At present there is no algorithm to correct the data so the bad data are marked with E_quality<=1 and bit 11 in E_bitmask.

Since it is sometimes difficult to discern between these wakes and a real electric field, analysis of the electric field should be done with caution in regions where cold plasma ion drift occurs. Users should consider comparing such measurements to EDI data, which is not affected. When ASPOC is operating, the spacecraft potential is kept at a much lower value and the problem of wakes due to cold ion drift is much less severe. More information on these wakes can be found in Eriksson et al. [2006], Engwall et al. [2006], Bonnell et al. [2008], André et al. [2015] and in the CAA-EFW Calibration Report.

***Note*: The wake identification is performed automatically and may not always mark the entire interval.**

6.13 Plasmasphere wake (bit 12, E_quality<=1)

During comparisons of electric field measurements done by EFW and EDI in the inner magnetosphere, it was found that the EFW data sometimes measures a spurious field of the order of 1-2 mV/m, mostly in the sunward direction. The raw data signal is often non-sinusoidal. Some discussion of these fields is given in Puhl-Quinn et al. [2008]. For an example, see Figure 10 in the CAA-EFW Calibration Report.

The cause of this field is not yet fully understood, but an empirical algorithm has been developed to detect the bad data. The algorithm uses a comparison between the measured electric field and the expected field if the ambient plasma were to co-rotate with Earth, and is applied only in regions of high density as indicated by the spacecraft potential. There is no correction applied to the data, but they are marked with E_quality<=1 and bit 12 in E_bitmask. Users studying the electric field in the inner magnetosphere should be aware of this problem, since the detection is not always perfect.

6.14 WHISPER operating (bit 13, E_quality<=2)

The WHISPER instrument is an active sounder that uses the EFW probes for transmission and reception of the signals. The WHISPER pulses typically occur once every 52 or 104 seconds and are timed to interfere minimally with EFW operations. However, the plasma response to the WHISPER active stimulus may perturb the EFW measurements near the pulse.

The perturbations are particularly noticeable for measurements using the 180 Hz filter (i.e. all measurements at 450 Hz, all measurements on C2 after July 2001, and all measurements on all spacecraft after May 2015), and for measurements in the solar wind (i.e. in weak field). Consequently, the WHISPER sounding pulses are marked with bit 13 of E_bitmask, and E_quality is reduced to <=2. Often, this data is in fact of equal quality as the data around it. However, users should beware of any signals (spikes or waves) that repeat synchronously with the WHISPER soundings.

6.15 High bias saturation (bit 14, E_quality<=1)

As discussed in Section 5.1.5 , if the EFW instrument draws too large a bias current then the probes tend to shoot to large negative potentials (“saturate”). This happens on occasion when the plasma density is high. As an example, the problem was worse in 2005 and early 2006, and was largely eliminated by a change in the bias settings on 16 June 2006. See also the CAA-EFW Calibration Report. Similar problem reoccurred in 2015 and 2016. Intervals affected by high bias saturation exhibit large spin-synchronous spikes in the electric field data, and the data are effectively useless. This is marked with bit 14 of E_bitmask.

Bit 14 is also set whenever the probe-to-spacecraft potential becomes positive (i.e. Vsc<0). Under such conditions, the probe biasing cannot be expected to effectively anchor the probes to the local plasma potential. In effect, the probe bias current becomes too large as a result of changes in the plasma. Although large spin-synchronous spikes may not be present in such cases, the data should be treated with extreme caution.

6.16 Bias current DAC not responding correctly (bit 15, E_quality<=2)

This bit indicates that the EFW bias setting is not the commanded one, so that the electric field measurement is not optimal. Sometimes this happens after a bias sweep, when the bias gets stuck at some value.

6.17 Probe shadow saturation (bit 16, L2 E_quality<=1)

This bit indicates the times when one of the EFW probes relevant to a measured signal saturates due to a shadow from the spacecraft or EFW preamplifier housing (the "puck"). In nominal operation mode the EFW probes are operated in such a way that the photoelectron current from the probe is balanced by the bias current applied to the probe. A probe going into full or partial shadow means reduced photo emission. In such a situation the applied bias current can no longer be balanced, leading to the probe getting charged to a large negative potential. Electric field measurements are not possible under such conditions.

Since May 2014 the spacecraft spin axis is not adjusted to avoid shadow on the probes. From this time shadow on each probe during a small part of the spacecraft spin is the common situation.

Figure 10 below shows electric field measurements from probe pair 12 with probes 1 and 2 experiencing shadow once per spin. The shadow periods can be clearly seen in the plot as large spikes in the electric field. The blue parts of the curve correspond to the time during which the bit is set. The red parts of the curve show time intervals during which the electric field measurement is not affected by shadows (bit 16 not set).

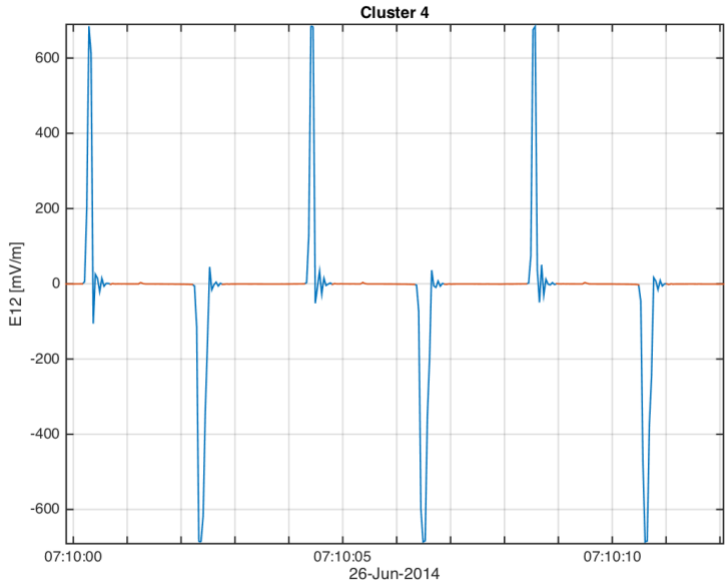

Figure 10: Probes saturation due to shadowing by the spacecraft or the EFW preamplifier housing (the "puck") .

7 How to acknowledge the use of EFW data

When using EFW data in a scientific publication or presentation, please acknowledge the EFW team and include the EFW DOI (Digital Object Identifier): https://doi.org/10.5270/esa-rp1zebe

This is a unique identifier of EFW data that will not change over time.

As an example you can include the following in the publication acknowledgements: We thank the team providing data from the EFW instrument (doi: 10.5270/esa-rp1zebe) on the ESA Cluster spacecraft.

8 References

8.1 Other applicable CAA-EFW documents

The CAA-EFW calibration report

> Khotyaintsev, Y., Calibration Report of the EFW Measurements in the Cluster Active Archive (CAA).
>
> https://www.cosmos.esa.int/web/csa/documentation

contains useful information regarding problems and calibration of the CAA data.

The formal document describing the EFW data delivery to CAA is

> Lindqvist, P.-A., and Y. Khotyaintsev, Cluster Active Archive: Interface Control Document for EFW, ESA document CAA-EFW-ICD-0001.
>
> https://www.cosmos.esa.int/web/csa/documentation

The Users Guide to the Cluster Science Data System contains information regarding parameters in the CSDS system.

> https://www.cosmos.esa.int/web/csa/documentation

8.2 Other online information

The Cluster Science Archive is available at

> https://www.cosmos.esa.int/web/csa

General information on the EFW instrument can be found on the EFW home page at

> http://www.cluster.irfu.se

Information on EFW operations, both standard operations and anomalies (including detailed information on commissioning, calibrations, bias settings, internal burst operations and sweep operations), can be found on the EFW operations home page at

> http://www.cluster.irfu.se/efw/ops

A chronological table of all non-standard operations and known instrument anomalies is available at

> http://www.cluster.irfu.se/efw/ops/ns_ops.html

8.3 Printed information

The EFW instrument description is in

Gustafsson, G., R. Boström, B. Holback, G. Holmgren, A. Lundgren, K. Stasiewicz, L. Åhlén, F. S. Mozer, D. Pankow, P. Harvey, P. Berg, R. Ulrich, A. Pedersen, R. Schmidt, A. Butler, A. W. C. Fransen, D. Klinge, M. Thomsen, C.-G. Fälthammar, P.-A. Lindqvist, S. Christenson, J. Holtet, B. Lybekk, T. A. Sten, P. Tanskanen, K. Lappalainen, and J. Wygant, The Electric Field and Wave Experiment for the Cluster Mission, Space Sci. Rev., **79**, 137-156, 1997.

and is further elaborated and updated in

Gustafsson, G., M. André, T. Carozzi, A.I. Eriksson, C.-G. Fälthammar, R. Grard, G. Holmgren, J.A Holtet, N. Ivchenko, T. Karlsson, Y. Khotyaintsev, S. Klimov, H. Laakso, P.-A. Lindqvist, B. Lybekk, G. Marklund, F. Mozer, K. Mursula, A. Pedersen, B. Popielawska, S. Savin, K. Stasiewicz, P. Tanskanen, A. Vaivads, and J.-E. Wahlund, First results of electric field and density observations by Cluster EFW based on initial months of operation., Ann. Geophys., 19, 1219-1240, 2001.

Detailed information about the characteristics of the EFW analogue filters can be found in

G. Stenberg, Cluster EFW Filter Calibration Report, 2002.

https://www.cosmos.esa.int/web/csa/documentation

A short overview of the EFW data in CAA can be found in

Lindqvist, P.-A., Y. Khotyaintsev, M. André, and A. I. Eriksson, EFW data in the Cluster Active Archive, in Proc. Cluster and Double Star Symposium – 5th Anniversary of Cluster in Space, Noordwijk, The Netherlands, 19-23 September 2005, **ESA SP-598**, 5 pp., 2006.

https://www.cosmos.esa.int/web/csa/documentation

Khotyaintsev, Y., P.-A. Lindqvist, A. I. Eriksson and M. André, The EFW Data in the CAA, The Cluster Active Archive, Studying the Earth's Space Plasma Environment. Edited by H. Laakso, M.G.T.T. Taylor, and C. P. Escoubet. Astrophysics and Space Science Proceedings, Berlin: Springer, p.97-108, doi:10.1007/978-90-481-3499-1_6, 2010.

A description of the solar wind wakes and their removal is found in

Eriksson, A. I., Y. Khotyaintsev, and P.-A. Lindqvist, Spacecraft wakes in the solar wind, in Proc. 10th Spacecraft Charging Technology Conference (SCTC-10), Biarritz, France, 18-21 June 2007 (also available as http://space.irfu.se/aie/publ/Eriksson2007b.pdf).

André, M. A. I. Eriksson, Y. V. Khotyaintsev and S. Toledo-Redondo, The spacecraft wake: Interferece with electric field observations and a possibility to detect cold ions, J. Geophys. Res., Space Physics, **126,** e2021JA029493,doi:10.1029/2021JA029493, 2021.

A description of the characteristics of lobe/polar wind wakes is found in

A. I. Eriksson, M. André, B. Klecker, H. Laakso, P.-A. Lindqvist, F. Mozer, G. Paschmann, A. Pedersen, J. Quinn, R. Torbert, K. Torkar, and H. Vaith, Electric field measurements on Cluster: comparing the double-probe and electron drift techniques, Ann. Geophysicae, **24**, 275-289, SRef: 1432-0576/ag/2006-24-275, 2006,

with detailed simulations presented by

E. Engwall, A. I. Eriksson and J. Forest, Wake formation behind positively charged spacecraft in flowing tenuous plasmas, Phys. Plasmas, **13**, 062904, doi: 10.1063/1.2199207, 2006.

Some discussion of the lobe wakes in the context of THEMIS is also contained in section 4.5 of

J.W. Bonnell, F.S. Mozer, G.T. Delory, A.J. Hull, R.E. Ergun, C.M. Cully, V. Angelopoulos and P.R. Harvey, The Electric Field Instrument (EFI) for THEMIS, Space Sci. Rev., doi:10.1007/s11214-008-9469-2, 2008.

A useful reference regarding the spurious fields in the inner magnetosphere is

P.A. Puhl-Quinn, H. Matsui, V.K. Jordanova, Y. Khotyaintsev and P.-A. Lindqvist, An effort to derive an empirically based, inner-magnetospheric electric field model: Merging Cluster EDI and EFW data, J. Atmos. Sol-Terr. Phys., doi:10.1016/j.jastp.2007.08.069, 2008.

How the spacecraft potential is used to determine plasma density is discussed in

Pedersen, A., B. Lybekk, M. André, A. Eriksson, A. Masson, F. S. Mozer, P.-A. Lindqvist, P. M. E. Décréau, I. Dandouras, J.-A. Sauvaud, A. Fazakerley, M. Taylor, G. Paschmann, K. R. Svenes, K. Torkar, and E. Whipple, Electron density estimations derived from spacecraft potential measurements on Cluster in tenuous plasma regions, J. Geophys. Res., **113**, A07S33, doi: 10.1029/2007JA012636, 2008.

Lybekk, B., A. Pedersen, S. Haaland, K. Svenes, A. N. Fazakerley, A. Masson, M. G. G. T. Taylor, and J.-G. Trotignon, Solar cycle variations of the Cluster spacecraft potential and its use for electron density estimations, J. Geophys. Res., **117**, A01217, doi:10.1029/2011JA016969, 2012.

André, M., K. Li and A. I. Eriksson, Outflow of low energy ions and the solar cycle, J. Geophys. Res., Space Physics, **120**, 1072–1085, doi:10.1002/ 2014JA020714, 2015.

Andriopoulou, M., R. Nakamura, K. Torkar, W. Baumjohann and B. Hoelzl, Deriving plasma densities in tenuous plasma regions, with the spacecraft potential under active control, J. Geophys. Res., Space Physics, **120,** 9594–9616, doi:10.1002/2015JA021472, 2015.

Roberts, O. W., R. Nakamura, K. Torkar, D. B. Graham, D. J. Gershman, J. C. Holmes, A. Varsani, C. P. Escoubet, Z. Vörös, S. Wellenzohn, Y. Khotyaintsev, R. E. Ergun and B. L. Giles, Estimation of the electron density from spacecraft potential during high-frequency electric field fluctuations, J. Geophys. Res., Space Physics, **125**, e2020JA027854, doi:10.1029/2020JA027854, 2020.

The results of simulations of the electrostatic potential around the spacecraft and how the electric field measurements are affected may be found in

Cully C. M., R. E. Ergun, and A. I. Eriksson, Electrostatic structure around spacecraft in tenuous plasmas, J. Geophys. Res., **112**, A09211, doi:10.1029/2007JA012269, 2007.

Appendix A. Processing details

A.1. Least squares fits and raw data offsets

In the presence of a constant ambient electric field, the raw data signal is a sine wave where the amplitude and phase of the sine wave give the electric field magnitude and direction. Theoretically, the DC level of the raw data should be zero. But small differences between the probe surfaces and in the electronics create a DC offset in the raw data. If uncorrected, this DC offset would show up in the de-spun electric field data as a signal at the spin frequency.

The least-squares fits done on the raw data serve two purposes. Firstly, it gives a measurement of the electric field at the spin resolution, where only one probe pair is necessary. Secondly, it gives a possibility to find the DC raw data offset, which can then be used to correct the raw data before despinning the full resolution electric field. A least-squares fit to the raw data of the form

$$y = A + B \sin(\omega t) + C \cos(\omega t) + D \sin(2\omega t) + E \cos(2\omega t) + ...$$

where ω is the spin frequency (and calculated from the sun reference pulse), is done once every 4 seconds, and gives the following output:

- The sine and cosine terms, B and C (the electric field)
- The DC offset, A
- The standard deviation of the raw data from the fitted sine wave, σ
- Higher order terms, D, E, ..., may be used for diagnostics of data quality

During this fitting, outliers are iteratively discarded by removing points more than 3σ from the curve and then re-fitting. At most 10 such iterations are performed.

The electric field (computed from B and C) and the standard deviation σ are directly input to the CAA as L3_E (see Section 4.4). There are small differences in the DC level of the raw data (A) from one spin to another, mainly because of real variations in the electric field. Therefore the DC offset is smoothed before using in the Level 2 processing using a weighted average over 7 spins; the averaged offset is then used for processing the Level 2 data and is archived as the ancillary data product C[n]_CP_EFW_L3_DER (Section 4.7).

A.2. Sunward DC offsets and amplitude correction

After despinning, the electric field data (both Level 2 and Level 3) give the electric field as measured by the EFW instrument. This field contains some systematic errors, which need to be corrected for, namely an amplitude correction and DC offset removal.

The spacecraft potential, which is also the potential of the wire booms, extends out to a large distance from the spacecraft. The ambient electric field is thus "short-circuited" by the presence of the spacecraft and wire booms, so the EFW instrument measures only a certain fraction of the real ambient electric field. By simulations and comparisons with other data (mainly CIS), it has been determined that the measured electric field magnitude needs to be multiplied by a factor of 1.1 to get the real electric field (see also CAA-EFW Calibration Report, and Cully et al., 2007). The same value is used for all spacecraft and for the entire mission.

The spacecraft, wire booms and probes emit photoelectrons, which create a cloud of excess negative charge around the system, mainly on the sunward side. This will be measured by the EFW instrument as a spurious sunward electric field, generally referred to as the sunward offset, which needs to be subtracted from the data. The magnitude of this sunward offset is determined by comparisons with other instruments, mainly EDI and CIS. The offset varies slowly with time, with plasma region, and is slightly different for the different spacecraft. This offset is removed from the data before delivery to CAA. The value of the offset that have been subtracted from the data are given in the file_caveats section in the header of the CEF file (look for "ISR2 offsets").

The photoelectron asymmetry responsible for the sunward offset by definition gives an offset in the sunward direction only. However, results of comparisons with other instruments have at times shown a small offset also in the duskward (Ey) direction, which is not yet well understood.

Appendix B. Probe bias, puck and guard settings

The EFW instrument hardware is briefly described in section 2.1. Table 10 gives an overview of the settings of the currents used to bias the individual probes, and the voltages used to bias the corresponding puck and guard.

Table 10 provides an overview of periods with mainly constant settings over longer periods. Shorter periods with alternative settings can occur at any time due to tests or minor operational problems. For detailed studies the instrument settings provided in the EFW housekeeping data set should be used (see Table 7).

C1

Date	Mode	Bias				Puck				Guard			
010101	EEEE	-180nA	-180nA	-220nA	-220nA	-1V	-1V	-1V	-1V	-6V	-6V	-6V	-6V
010124	EEEE	-180nA	-180nA	-220nA	-220nA	-1V	-1V	-1V	-1V	-6V	-6V	-6V	-6V
010425	EEEE	-180nA	-180nA	-180nA	-180nA	-1V	-1V	-1V	-1V	-6V	-6V	-6V	-6V
010526	EEEE	-180nA	-180nA	-180nA	-180nA	+1V	+1V	+1V	+1V	-6V	-6V	-6V	-6V
011228	**p1 failure**												
020108	DEEE	0	-140nA	-140nA	-140nA	-1V	-1V	-1V	-1V	-6V	-6V	-6V	-6V
020111	DEEE	0	-140nA	-140nA	-140nA	0	+1V	+1V	+1V	0	-6V	-6V	-6V
060617	DEEE	0	-100nA	-100nA	-100nA	0	+1V	+1V	+1V	0	-6V	-6V	-6V
091014	**p4 failure**												
091028	DEED	0	-100nA	-100nA	0	0	+1V	+1V	0	0	-6V	-6V	0
111010	DEED	0	-140nA	-140nA	0	0	+1V	+1V	0	0	-6V	-6V	0
121106	DEED	0	-140nA	-140nA	0	0	+1V	+1V	0	0	-3.7V	-3.7V	0
161128	DEED	0	-100nA	-100nA	0	0	+1V	+1V	0	0	-3.7V	-3.7V	0
180222	DEED	0	-140nA	-140nA	0	0	+1V	+1V	0	0	-3.7V	-3.7V	0
180311	DEED	0	-100nA	-100nA	0	0	+1V	+1V	0	0	-3.7V	-3.7V	0
181210	**p3 failure**												
231224	DEDD	0	-100nA	0	0	0	+1V	0	0	0	-3.7V	0	0

C2

Date	Mode	Bias				Puck				Guard			
010101	EEEE	-180nA	-180nA	-220nA	-220nA	-1V	-1V	-1V	-1V	-6V	-6V	-6V	-6V
010110	EEEE	-180nA	-180nA	-180nA	-180nA	-1V	-1V	-1V	-1V	-6V	-6V	-6V	-6V
010123	EEEE	-180nA	-180nA	-220nA	-220nA	-1V	-1V	-1V	-1V	-6V	-6V	-6V	-6V
010425	EEEE	-180nA	-180nA	-180nA	-180nA	-1V	-1V	-1V	-1V	-6V	-6V	-6V	-6V
010601	EEEE	-140nA	-140nA	-140nA	-140nA	+1V	+1V	+1V	+1V	-6V	-6V	-6V	-6V
060617	EEEE	-100nA	-100nA	-100nA	-100nA	+1V	+1V	+1V	+1V	-6V	-6V	-6V	-6V
070513	**p1 failure**												
070623	DEEE	0	-100nA	-100nA	-100nA	0	+1V	+1V	+1V	0	-6V	-6V	-6V
1104	**low perigees**												
110430	DEEE	0	-20nA	-20nA	-20nA	0	+1V	+1V	+1V	0	-6V	-6V	-6V
121106	DEEE	0	-20nA	-20nA	-20nA	0	+1V	+1V	+1V	0	-3.7V	-3.7V	-3.7V
151012	**p2 failure**												
220823	**p3 failure**												
231217	DDDE	0	0	0	-20nA	0	0	0	+1V	0	0	0	-3.7V

C3

Date	Mode	Bias				Puck				Guard			
010101	EEEE	-180nA	-180nA	-220nA	-220nA	-1V	-1V	-1V	-1V	-6V	-6V	-6V	-6V
010109	EEEE	-180nA	-180nA	-180nA	-180nA	-1V	-1V	-1V	-1V	-6V	-6V	-6V	-6V
010124	EEEE	-180nA	-180nA	-220nA	-220nA	-1V	-1V	-1V	-1V	-6V	-6V	-6V	-6V
010424	EEEE	-180nA	-180nA	-180nA	-180nA	-1V	-1V	-1V	-1V	-6V	-6V	-6V	-6V
010526	EEEE	-180nA	-180nA	-180nA	-180nA	+1V	+1V	+1V	+1V	-6V	-6V	-6V	-6V
020729	**p1 failure**												
020811	DEEE	0	-140nA	-140nA	-140nA	0	+1V	+1V	+1V	0	-6V	-6V	-6V
060617	DEEE	0	-100nA	-100nA	-100nA	0	+1V	+1V	+1V	0	-6V	-6V	-6V
110601	**p3 failure**												
111010	DEEE	0	-140nA	-140nA	-140nA	0	+1V	+1V	+1V	0	-6V	-6V	-6V
121106	DEEE	0	-140nA	-140nA	-140nA	0	+1V	+1V	+1V	0	-3.7V	-3.7V	-3.7V
141103	**p2 failure**												
150407	DDEE	0	0	-140nA	-140nA	0	0	+1V	+1V	0	0	-3.7V	-3.7V
161128	DDEE	0	0	-100nA	-100nA	0	0	+1V	+1V	0	0	-3.7V	-3.7V
170217	DDEE	0	0	-140nA	-140nA	0	0	+1V	+1V	0	0	-3.7V	-3.7V
170308	DDEE	0	0	-100nA	-100nA	0	0	+1V	+1V	0	0	-3.7V	-3.7V
180224	DDEE	0	0	-140nA	-140nA	0	0	+1V	+1V	0	0	-3.7V	-3.7V
180311	DDEE	0	0	-100nA	-100nA	0	0	+1V	+1V	0	0	-3.7V	-3.7V
240428	**p4 failure**												

C4

Date	Mode	Bias				Puck				Guard			
010101	EEEE	-180nA	-180nA	-220nA	-220nA	-1V	-1V	-1V	-1V	-6V	-6V	-6V	-6V
010109	EEEE	-180nA	-180nA	-180nA	-180nA	-1V	-1V	-1V	-1V	-6V	-6V	-6V	-6V
010124	EEEE	-180nA	-180nA	-220nA	-220nA	-1V	-1V	-1V	-1V	-6V	-6V	-6V	-6V
010425	EEEE	-180nA	-180nA	-180nA	-180nA	-1V	-1V	-1V	-1V	-6V	-6V	-6V	-6V
010601	EEEE	-140nA	-140nA	-140nA	-140nA	+1V	+1V	+1V	+1V	-6V	-6V	-6V	-6V
060617	EEEE	-100nA	-100nA	-100nA	-100nA	+1V	+1V	+1V	+1V	-6V	-6V	-6V	-6V
111012	EEEE	-140nA	-140nA	-140nA	-140nA	+1V	+1V	+1V	+1V	-6V	-6V	-6V	-6V
121027	EEEE	-140nA	-140nA	-140nA	-140nA	+1V	+1V	+1V	+1V	-3.7V	-3.7V	-3.7V	-3.7V
130701	**p4 failure**												
150217	**p3 bias failure**												
150505	EEED	-140nA	-140nA	-140nA	+4.5V	+1V	+1V	+1V	+1V	-3.7V	-3.7V	-3.7V	-3.7V
160203	EEED	-140nA	-140nA	-140nA	0	+1V	+1V	+1V	+1V	-3.7V	-3.7V	-3.7V	-3.7V
161128	EEED	-100nA	-100nA	-100nA	0	+1V	+1V	+1V	+1V	-3.7V	-3.7V	-3.7V	-3.7V
170217	EEED	-140nA	-140nA	-140nA	0	+1V	+1V	+1V	0	-3.7V	-3.7V	-3.7V	0
170307	EEED	-100nA	-100nA	-100nA	0	+1V	+1V	+1V	+1V	-3.7V	-3.7V	-3.7V	-3.7V
180222	EEED	-140nA	-140nA	-140nA	0	+1V	+1V	+1V	0	-3.7V	-3.7V	-3.7V	0
180311	EEED	-100nA	-100nA	-100nA	0	+1V	+1V	+1V	+1V	-3.7V	-3.7V	-3.7V	-3.7V

Table 10: Overview of Cluster 1-4 (C1-4) settings over periods with mainly constant parameters over longer periods. Shorter periods with alternative settings can occur at any time. The parameters are the probe bias currents (Bias) and puck and guard voltages (Puck, Guard). The mode of operation for the individual probes is also indicated (Mode) as electric field mode with a negative probe bias current (E) or voltage bias (D).